SANDIA REPORT
SAND2002-1045
Unlimited Release
Printed April 2002

Semiconductor Bridge Characterization and Explosive Component Development

Robert W. Bickes, Jr., Stuart A. Smith, W. Gary Rivera, Anita M. Renlund, Jill C. Miller, Daniel J. Savignon, and Bernardo Martinez-Tovar

Prepared by
Sandia National Laboratories
Albuquerque, New Mexico 87185 and Livermore, California 94550

Sandia is a multiprogram laboratory operated by Sandia Corporation, a Lockheed Martin Company, for the United States Department of Energy under Contract DE-AC04-94AL85000.

Sandia National Laboratories

Issued by Sandia National Laboratories, operated for the United States Department of Energy by Sandia Corporation.

SAND 2002-1045
Unlimited Release
Printed April 2002

Semiconductor Bridge Characterization and Explosive Component Development

Cooperative Research and Development Agreement, CRADA, Between Sandia National Laboratories and The Ensign-Bickford Company (Agreement 1540.0)

Robert W. Bickes Jr.
Power Source Components Department

Stuart A. Smith and W. Gary Rivera
Explosive Components Department

Anita M. Renlund and Jill C. Miller
Explosive Projects/Diagnostics Department

Daniel J. Savignon†
Analog Microelectronics Department

Sandia National Laboratories
P.O. Box 5800
Albuquerque, NM 87185-0614

Bernardo Martinez-Tovar
Semiconductor Bridge Technologies, Inc.
Albuquerque, NM 87106-4302

Abstract Follows

†Present Address: Analog Devices Inc., 7910 Triad Center Drive, Greensboro, NC 27409-9605

Abstract

The purpose of this CRADA was to: 1) demonstrate improved processing of the MC4217 by incorporation of a semiconductor bridge (SCB) initiator; 2) understand the fundamental processes of SCB initiation and energy transfer; and 3) develop smart SCB components for DOE/DP and commercial applications. For Task 1 we successfully demonstrated that we could incorporate an SCB into the MC4217 using modern bonding techniques that are employed in the semiconductor industry eliminating the present bottleneck in the processing the MC4217. For Task 2 we performed spectroscopic studies of the SCB/energetic material interface and observed the transfer of electronic energy from the SCB plasma directly into energetic materials with heavy metal atoms (BNCP, CP and ZPP). Tests on the pyrotechnic mix THKP were inconclusive, but electronic energy transfer did not appear to be a dominant mechanism. For Task 3 we designed and built a die containing an SCB, an explosive powder sensor and a cracked–die sensor. Sandia/DOE/government benefits include: a significant improvement in the production of the MC4217 by removing a major processing bottleneck; a fundamental understanding of the initiation mechanisms in SCB devices as well as data for modeling SCB behavior; a capability demonstration of MEMS technology; and employment of sunrise technologies to produce sophisticated WR components. For the Ensign–Bickford Company (EBCo) this CRADA provides them state of the art explosive component designs applicable for commercial market segments such as rock blasting and air bags and allows them the opportunity to be first to market with a smart explosive component. For the public SCB components offer improved components for air bags and seat belt restraints and techniques for rock blasting that will minimize ground shock, vibration and fly rock.

Acknowledgements

As project leader I want to thank all those who participated in this CRADA project. In particular I want to acknowledge our CRADA partners, the Ensign-Bickford Company (EBCo) and Semiconductor Bridge Technologies Inc. Many of their staff were active participants and they included EBCo staff members. Paul Marshall, and Mike Glessio and SCBT staff Marty Foster and Bernardo Martinez-Tovar.

Thanks also to my to my Sandia colleagues who participated including Stuart Smith, Gary Rivera, Dave Wackerbarth, William Tarbell, Anita Relund, Jill Miller, Dan Savignon, Wilson Barnard, Reid Bennett, Floyd Braaten, Greg Scharrer and Sheri Martinez. With apologies to those who I may have inadvertently omitted, and my thanks to everyone for their assistance to what I believe was a successful project.

Bob Bickes, September 2001.

CONTENTS

FIGURES

TABLES

NONMENCLATURE

1A/1W	No-fire requirement where a one-amp current passing through a 1-Ohm bridge for five minutes will not result in function. The 1A/1W no-fire requirement is driven by exposure to electromagnetic radiation (EMR)
BNCP	Explosive (2-(5-nitro-tetrazolato)tetramine cobalt(III) perchlorate)
CDU	Capacitive Discharge Unit
CP	Explosive (1-(5-cyanotretrazolato)pentaamine cobalt(III) perchlorate)
DDT	Deflagration-to-detonation
EBCO	The Ensign–Bickford Co.
EBW	Exploding Bridgewire
EMR	Electromagnetic radiation
ESD	Electrostatic Discharge - a pulse delivered to the bridge to simulate the discharge that might be obtained from the human body
HMX	Explosive [Cyclotetramethylene Tetranitramin]
PETN	Explosive [Pentaerythritol Tetranitrate]
PMMA	Plexiglas [Polymethylmethacrylate]
SCB	Semiconductor Bridge
SCBT	SCB Technologies, Inc.
SEM	Scanning Electron Microscope
THKP	Pyrotechnic (Titanium subhydride potassium perchlorate),
Time-To-Burst	Time from zero current to bridge burst
TMD	Theoretical Maximum Density
TOAD	Time of Arrival Detector
VISAR	Velocity Interferometer System for Any Reflector
ZPP	Pyrotechnic (Zirconium potassium perchlorate)

(THIS PAGE INTENTIONALLY LEFT BLANK)

SEMICONDUCTOR BRIDGE CHARACTERIZATION AND EXPLOSIVE COMPONENT DEVELOPMENT

Robert W. Bickes, Jr.
Sandia National Laboratories
P.O. Box 5800
Albuquerque, NM 87185-0614

1.1 - BACKGROUND

Currently explosive components like the MC4217 employ small metal wires that must be tediously attached to the component by hand for which manufacturing companies often have only one or two staff that can carry out the process. In addition, modeling of explosive components is difficult because details of the initiation process are not well known. Finally, conventional explosive technologies cannot meet today's sophisticated demands for government or commercial applications. For these reasons this project was undertaken because we felt that semiconductor bridge, SCB, devices could overcome each of these obstacles to improve explosive components and our understanding of explosive phenomena. The SCB is a Sandia patented technology licensed by the Ensign-Bickford Company, EBCo, a supplier of MDE components to Sandia and a manufacturer of commercial explosive devices.

1.2 - DESCRIPTION

Our objectives were to improve the processing of the MC4217, obtain a fundamental understanding of the SCB initiation mechanism, and develop a smart explosive component concept. EBCo and SCB Technologies, SCBT, staff developed the procedures to bond the SCB chip to the MC4217 for Task 1 and provided components for testing, processed the SCB die and provided devices for the tests for Task 2, suggested criteria for smart SCB commercial components and advised Sandia on technical issues for Task 3. Sandia staff tested and determined the design parameters for an SCB/MC4217, carried out the optical experiments and analyzed the data for Task 2, and designed, built and tested the components for Task 3.

1.3 - BENEFITS TO THE DEPARTMENT OF ENERGY

This project demonstrated that sunrise technologies are available for components for future weapon architectures. It provided the first step on the way to development of a smart explosive component utilizing MEMS technology as well as data that will provide fundamental insights into the initiation of explosive materials.

1.4 - ECONOMIC IMPACT

The decision to employ the SCB/MC4217 will lie with Sandia systems organizations. The new component eliminates the time consuming processing bottleneck of the present design; further it affords EBCo better utilization of its production staff because the attachment process does not require highly skilled personnel. The SCB/MC4217 concept also provides EBCo with an opportunity to compete in the commercial exploding bridgewire market utilizing this new idea. The development of the smart SCB was hindered by the shutdown of Sandia IMEMS processing; nonetheless, this project demonstrated that circuitry and the SCB can be incorporated on the same die and that the die can withstand the loading of explosive powder at high pressures. This is the first step towards the design of a fully integrated chip, which can lead to a wide variety of components for both government and commercial applications, specifically, advanced aerospace ordnance systems and smart air bag components for advanced automobile safety systems.

1.5 - PROJECT STATUS

This project was completed on April 22, 2001.

2.0 Task 1: Retrofit of an MC4217 Detonator with an SCB

Stuart A. Smith, W. Gary Rivera
Sandia National Laboratories
P.O. Box 5800
Albuquerque, NM 87185-0614

Bernardo Martinez -Tovar
Semiconductor Bridge Technologies, Inc.
1009 Bradbury Drive S.E.
Albuquerque, NM 87106-4302

Abstract

Currently, the MC4217 Detonator program utilizes exploding bridgewire (EBW) igniters to initiate the CP initial pressing, which, in turn, initiates the HMX output charge. The present method of welding the 0.001" diameter bridgewire for the MC4217 Detonator is resistance welding. This resistance welding technique requires specially trained personnel. Typically, these trained personnel are rare, sometimes being the sole person in the company qualified to do this task. This presents a significant bottleneck in the manufacturing process of these, and other, initiators.

An alternative to using an EBW initiator in the MC4217 detonator, and a solution to the bottleneck issue, is to use SCB initiator technology. To accomplish this design change, the SCB would be epoxy mounted to the header with 0.005" diameter wire leads ultrasonically welded to the lands on the chip and the header electrodes. The ultrasonic welding technique is significantly easier to master, thus allowing multiple personnel to be qualified to complete this process. In fact, the ultrasonic welding technique is widely used and accepted in the semiconductor industry.

The MC4217 EBW Detonator used in the Stockpile has a function time specification of 2.03 μs to 2.23 μs with a range within the lot of no greater than 0.120 μs. Experiments completed and detailed in this report, indicate the SCB version of the MC4217 using CP had a mean function time of 3.761 μs with a range of 1.118 μs. Experiments indicated the SCB version of the MC4217 using BNCP had a mean function time of 1.552 μs with a range of 0.116 μs.

The SCB with perpendicular orientation (see body for description) and low density powders, approximately one half the TMD, proved the combination to provide the best function times. For this reason, the perpendicular orientation using the given firing set parameters, would be the recommended SCB configuration for future experiments.
It was proven that CP and BNCP will DDT with SCB initiation but more work is needed on powder morphology. Optimizing the powder for SCB applications is necessary before

the SCB can be incorporated into the MC4217. Judging from experimental data, the BNCP powder looks to be more promising for SCB applications than CP powder.

Finally, the goal of this work was to provide a reliable, fieldable, and cost effective SCB MC4217 with which the change will be transparent to the system end user. While there is still work to do in the areas of SCB chip optimization, explosive powder density and morphology, and reliability to meet tactical requirements, we feel confident that these challenges are achievable.

2.1 - INTRODUCTION

Sandia National Laboratories developed the Semiconductor Bridge (SCB) igniter for the ignition of a variety of explosive materials. When subjected to a low energy current pulse (less then 3 millijoules), the bridge bursts into a plasma causing rapid ignition of the explosive material pressed against the bridge. Despite the low energies required for ignition, SCB components can be constructed to be explosively safe, meeting both electrostatic discharge (ESD) and no-fire requirements.[1] In addition, because heat transfer into the powder is a convective process, explosive outputs are obtained on a microsecond time scale. Finally, because SCB devices are processed using standard semiconductor fabrication techniques, circuitry on the same chip as the SCB can be incorporated for enhanced ESD, no-fire protection, precise timing delays, and logic for computer control. These "smart" SCB devices can be used for applications that include severe environments, precise timing for delays or sequencing, response to coded signals, and very low energy inputs.

Currently, the MC4217 Detonator program utilizes an Exploding Bridgewire (EBW) to initiate the CP initial pressing, which, in turn, initiates the HMX output charge, as shown in Appendix A. See Fig. 2-1 for a cutaway of the MC4217. The present method of welding the 0.001" diameter bridgewire for the MC4217 Detonator is resistance welding. This resistance welding technique requires specially trained personnel. Typically, these trained personnel are rare, occasionally being the sole person in the company qualified to do this task. This presents a significant bottleneck in the manufacturing process of these, and other, conventional bridgewire initiators.

An alternative solution to the bottleneck issue associated with an EBW initiator in the MC4217 detonator is to use SCB initiator technology. To accomplish this design change, the SCB would be epoxy mounted to the header and 0.005" diameter wire leads ultrasonically welded to the lands on the chip and the header electrodes. The ultrasonic welding technique is significantly easier to master, thus allowing multiple personnel to be qualified to complete this process. In fact, the ultrasonic welding technique is widely used and accepted in the semiconductor industry.

Replacing the resistance welding of the bridgewire with an SCB using ultrasonic welding would reduce the cost and risk to the MC4217 program. In addition, the effect to the end user would be transparent.

This report covers Task 1 of the CRADA, where extensive tests were done to show performance characteristics of the SCB devices were compatible with system requirements of the MC4217 Detonator.

2.2 – SCOPE OF WORK

The goal of Task 1 is to demonstrate that the replacement of the exploding bridgewire in an MC4217 detonator with an SCB satisfies the following criteria:

(a) meets MC4217 performance requirements,
(b) improves the bonding process,
(c) meets 1A/1W no-damage levels, and
(d) operates with both CP or BNCP explosives in the deflagration-to-detonation (DDT) column.

Each task listed in Table 2-1 was accomplished either by Sandia, Semiconductor Bridge Technologies Inc. (SCBT), or the Ensign-Bickford Company (EBCo.) staff. This report is intended to satisfy Subtask 8 of the CRADA statement of work, and includes information from both Sandia National Laboratories activities and SCBT activities.

2.3 - RESULTS

2.3 - 1 Subtask 1: Design of a Low Resistance Die.

The resistance of any detonator bridge, whether it is an EBW or a SCB, affects the amount of energy that can be deposited into it. The more energy into the bridge, the quicker the initiation. Reducing the bridge resistance of the SCB would allow more energy to be deposited. The major factors which play a role in how much, and how fast, energy can be deposited into the bridge are the resistance, inductance, and capacitance of the firing set. Given that the typical SCB resistance (1 ohm) is three times larger than the MC4217 bridgewire resistance, Subtask 1 focused on the reduction of SCB resistance.

The resistance of the MC4217 bridgewire is 0.330 ± 0.020 Ohms. In contrast, the common practice has been to design SCBs with a resistance of 1.0 Ohm to duplicate the resistance of hot wire devices. This corresponds with the lowest nominal resistance for one of SCBT's off-the-shelf SCB devices, the model 3-2B1 SCB. The design resistance of the 3-2B1 SCB is 1.0 ± 0.010 Ohms.

The Type 3-2B1 SCB was chosen for the MC4217 Retrofit task. This design has undergone years of testing, has met the 1A/1W No-fire requirements as well as ESD requirements[1] and there exists substantial experimental data for this design. In addition, the chip is readily available as an "off-the-shelf" part.

A lower resistance version of the 3-2B1 SCB was built to yield a resistance of 0.75 ± 0.010 Ohm. This SCB was created by maximizing the impurity levels for doping of the polysilicon layer used to form the 3-2B1 bridge. Using the 3-2B1 SCB bridge geometry, the lowest resistance feasible without developing a completely new SCB with a larger bridge volume was 0.75 Ohm.

Figure 2-2 shows the proposed design of a new bridge with a diagonal configuration necessary to develop a bridge resistance of nominally 0.3 Ohms and fit between the MC4217's pins. The proposed bridge dimensions are length, L=75 μm, width, W=550 μm and thickness, Th=2 μm as compared to the 3-2B1 with dimensions of L=100 μm W=380 μm and Th=2 μm. The proposed design has a 6,500 μm^3 larger volume, which is necessary to reduce the bridge resistance at the standard doping level.

In order to determine the benefits of lowering the SCB resistance, testing was conducted with the 1.0 Ohm and 0.75 Ohm SCBs and the TC1061 Capacitor Discharge Unit (CDU). The TC1061 fire set simulator is used for production acceptance of the MC4217. This "high voltage" CDU was used to fire the SCBs, delivering an average power of 350 megawatts at 1150 volt charge.

The CDU's available power was large enough that the 1.0 Ohm resistance of the SCB did not significantly degrade the CDU's performance. The 0.75 Ohm SCB average time-to-burst was approximately 0.19 μs, with an energy at bridge burst of approximately 30 mJ. The average time-to-burst for the 1.0 Ohm SCB was also approximately 0.19 μs, with an energy of 30 mJ. An example of the timing, voltage, and current data taken for these tests is given in Fig. 2-3.

This experimental data indicate there were no differences in the mean "time-to-burst" and energy at burst between the 1.0 Ohm and 0.75 Ohm SCBs.

Conclusion: The experimental data indicates that there are no appreciable difference in CDU performance between the 1.0 Ohm and 0.75 Ohm SCB devices when mean "time-to-burst" and burst energy are considered. Function tests indicated little or no performance differences between the 1.0 Ohm SCB and the 0.75 Ohm SCB. The CDU contained excess energy and the 0.3 Ohm SCB would likely not provide enough benefit to justify the cost and time required for its development. Consequently, development of the 0.3 Ohm SCB was not pursued further.

2.3 – 2 Subtask 2: Preliminary Design Review of SCB Insertion Requirements

The Preliminary Design Review of SCB Insertion Requirements consisted of informal phone conversations with both EBCo and SCBT staff and in a meeting with Paul Marshall (EBCo) and Martin Foster (SCBT) on March 19, 1999.

2.3 – 3 Subtask 3: Process 3-2 and Low Resistance Die and Mount on TO46 Headers.

SCBT completed this work and a short synopsis is presented here. Reference 2 has more information.

In order to determine the effect of lower resistance SCB's needed for the MC4217 header initiator, a new batch of chips was manufactured at SCBT. Maximum doping level (saturation) conditions were used in the process of doping the polysilicon bridge, which yielded an average resistance of 0.75-Ohm. The bridge geometry and volume were maintained the same as the 1.0 Ohm SCB.

The 3-2B1 SCB chips were epoxy attached and wire bonded to conventional TO46 headers (better known as transistor cans) as shown in Figs. 2-4 and 2-5. This header has two, 0.020" diameter by 0.5" long leads. One lead is connected to the header's body and the other goes through the header and is isolated by a metal-to-glass seal. The header surface diameter, where the SCB die is mounted, is 0.200" diameter, and large enough that the size and placement of the SCB die was not critical.

Because of the relatively large header size, the 3-2B1 SCB chip was maintained with its nominal dimensions of 0.045" x 0.055" (1.14 mm x 1.40 mm), and typical wire bonding tooling and parameters, routinely used at SCBT, were used. One wire bond was connected between the SCB and the header's body, and the other between the SCB and the isolated lead, see Fig. 2-6. Brass charge holders were then epoxy attached to the TO46 headers in preparation for powder loading at Sandia.

2.3 – 4 Subtask 4: Characterize and Test SCB Die on TO46 Headers.

The purpose of Subtask 4 was to conduct a series of tests using the SCB die in order to characterize its performance in relation to the parameters of the MC4217.

The MC4217 design consists of an initial 0.183" long initial pressing of 1.0 g/cm^3 CP, pressed in a single increment, followed by a 0.047" long, 1.58 g/cm^3, HMX output pellet. The explosive column diameter is 0.095", and the length is 0.230". In comparison, the TO46 header is 0.150" in diameter and 0.270" long. A brass sleeve designed to mate with the TO46 header was epoxied to the header to hold the explosive charge. The geometry of the charge holder has an ID of 0.150", an OD of 0.250", and an internal length of 0.270". The test hardware used for SCB characterization is shown in Figs. 2-4 and 2-5.

Testing in Subtask 4 utilized the MC4217's TC1061 high voltage firing set. Given a capacitance of 0.4 μF, and a voltage of 1150 volts, the fire set is capable of delivering 264 mJ of energy. This energy is more than sufficient for SCB bridge burst.

Approximately 120 3-2B1 SCBs were processed for this CRADA, twenty of which were the low resistance (0.75 Ohm) SCBs.

Explosive Type and Particle Size

Explosive combinations considered for use with the SCB were BNCP/HMX, and CP/HMX. SCB testing has been done previously[3] with PETN pressed against the bridge at a density of 1.65 g/cm^3 . The high packing pressures were necessary because at lower packing pressures the powder could relax and shrink back away from the SCB bridge creating gap between the bridge and powder. Experimental data indicates no detonation would occur when gaps were present. Packing pressures and densities of the CP and BNCP were studied, and are reported later in Subtask 4.

In addition to explosive type, the effect of particle size of each explosive type was investigated. A characteristic of large particle powders is that they contain air voids in the interstitial spaces between the particles, as well as having lower surface areas. The interstitial voids make transmission of energy more difficult in these large particle powders. In addition, as the plasma from the SCB condenses on the surface of a large particle, it cannot cover enough of the surface to heat it to ignition temperatures, thus resulting in no ignition.

Scanning Electron Microscope (SEM) imagery was used to investigate the morphology of the explosive power used for this testing. SEM imagery for 2 μm particle size BNCP from Lot EL93347 is given in Fig. 2-10. Shown in Fig. 2-11 is 20μm BNCP from Lot EL94607. SEM photography of the even larger 100 μm particle size BNCP from Lot EL88461 is given in Fig. 2-12. The 50 μm to 100 μm CP of Lot EL82921 is given in Fig. 2-14. Batch 8 HMX powder is shown in Fig. 2-15. Both the CP and HMX power lots are currently being used in MC4217 production.

Due to the high energy output of the fire set, powder ignition was successful with each of the powder types/sizes, with the exception of the large 100 μm BNCP particles.

Parallel versus Perpendicular Orientation

It was observed in past experiments that parallel orientation (see following for definition) of the SCB with high density PETN and a high voltage firing set achieved detonation whereas the perpendicular orientation did not detonate. In the perpendicular orientation, the wires on the attachment lands of the SCB are located such that the current flow is perpendicular to the line drawn between the pins. Figure 2-6 shows the TO46 header with the 3-2B1 SCB mounted in the perpendicular orientation. In the parallel orientation, the SCB is rotated 90º, so that the current flow was along the line between the two electrodes. Attachment wires for both orientations consisted of 0.005” diameter aluminum wire.

Table 2-2 shows the difference in function times between the parallel and perpendicular SCB orientations. The SCBs tested with the parallel orientation yielded data with function times and standard deviations larger than the perpendicular orientation. For this reason, the perpendicular orientation was chosen for testing. In addition, the data also

provided information regarding the relationship between function times and powder densities. These data are plotted in Figs 2-7 and 2-8.

The relationship of powder density on ignition energy is such that lower powder densities require higher ignition energies and visa versa. However, at sufficiently low densities, no-fires have been observed. [3]

CP Powder Density Study

The test data from the SCB orientation series indicated that, given the consistent use of the high voltage TC1061 CDU, powder density was a contributor to the SCB performance.

The density study consisted of pressing CP to four different densities (from 1.58 g/cm^3 to 1.96 g/cm^3), where the theoretical maximum density (TMD) for CP is 1.974 g/cm^3. The Explosive-Powder Compaction System[4] (Fixture ID #73) was used to compact the powder. Data from five tests at each of the four CP densities are given in Table 2-3. Data are also presented in Fig. 2-9.

In the parallel configuration the average function times for all four densities ranged between 5.090 μs to 6.028 μs and each had large standard deviations. From these data alone, the function timing trend appears to be influenced by packing pressure, where higher pressures result in lower function times. Although, the 40 kpsi units showed a lower average timing than the 50 kpsi units by 0.070 μs.

Earlier testing at 0.9 g/cm^3 and 1.0 g/cm^3 in the perpendicular configuration (see Fig. 2-8) showed function times in the 3.0 μs range. The density of the CP powder in the MC4217 is a nominal 1.0 g/cm^3, roughly one half TMD. To obtain 1.0 g/cm^3 density, the weight of CP in the TO46 header would be 76.5 mg and would require negligible packing pressure.

Given the CRADA goal of retrofitting the MC4217, it was decided to focus on simulating the MC4217's explosive column with either CP or BNCP and HMX explosives.

The density study is summarized in Appendix A.

MC4217 Explosive Column Simulation

Simulating the column length of the MC4217 required designing a pressing fixture for the CP that would stop at the correct height to achieve a 1.0 g/cc density. At this point, the HMX pellet was inserted. The MC4217 column diameter is 0.095". Because the 3-2B1 SCB and TO46 header pins would interfere with a second sleeve inserted into the brass sleeve in order to reduce the diameter to 0.095", simulating the column diameter was not

practical. Because all testing was consistent with respect to this geometry, column diameter would not invalidate test comparisons.

Data from this simulation are given in Table 2-4. Forty-three tests were conducted using CP/HMX and two BNCP/HMX explosive trains. Distinct differences between the three explosive powders were observed (see Figs. 2-10, 2-11, and 2-12), most notably between the two different particle sizes of BNCP, as can be seen in Fig. 2-13. Between these two powders, the 2 μm showed a longer function time and a standard deviation 11.5 times higher than the 20 μm powder. The differences between 20 μm BNCP and the CP powers were also significant (see Figs. 2-13 and 2-14). The CP units showed an average function time 1.84 times longer than the BNCP and a standard deviation 2.9 times greater.

Further research into optimizing BNCP particle morphology for SCB initiation was outside the scope of this CRADA, but is recommended. Figure 2-15 shows an SEM of HMX.

Subtask 4 Conclusions

The SCB testing explored the use of CP and BNCP of varying particle sizes and the orientation of the SCB on the header. The results showed the best function times were for a combination of perpendicular orientation, low density powders, and approximately one-half TMD.

A possible contribution to the consistently quicker function times of BNCP over CP is because the heat of reaction for BNCP is 1.05 kcal/g (or 4.4 kJ/g) and for CP it is 0.97 kcal/g (or 4.1 kJ/g). In addition, BNCP undergoes DDT more rapidly and in a shorter distance than CP.[5] Further study is recommended to gain a better understanding of the physics behind this powder initiation mechanism. A BNCP particle size optimization for the 3-2B1 SCB is also recommended.

2.3 – 5 Subtask 5: Develop Bonding Process to Attach SCB into MC4217 Detonators.

SCBT completed this work and a short synopsis is presented here. Reference [3] has more information.

The edge-to-edge pin spacing for the MC4217 header is 0.019" which is relatively small compared to the typical size of a standard SCB chip. The 3-2B1 SCB consists of a standard bridge design of the following geometry: L=100 μm, W=380 μm, and Th=2 μm. Nominal die size is of 0.045" x 0.055" x 0.020" thick. To accommodate this spacing, off-the-shelf 1.0-Ohm SCB chips were cut to a smaller die size (0.018"x0.055") in order to fit between the MC4217 contacts and be able to connect the wire bonds between the SCB die and the header's contacts. The SCB's wire bonding pads were trimmed while the

bridge material was not impacted in any way. The trimming of the die left ~0.0015" on each side of the bridge. This configuration is shown in Fig. 2-16.

Because of the space constraint between the SCB chip and the contacts of the MC4217 header, a special wire bonding technique was developed at SCBT in order to connect the wire bonds. This technique consisted of first epoxy attaching the SCB to the header. Next, by means of standard ultra-sonic wire bonding techniques, a 0.005" aluminum wire was first bonded to one of the SCB lands and then to the MC4217 header's pin. During the bonding process, the wire and header were manipulated in such a way that the bonded wire would form a loop without touching the side surface of the SCB die.

Electrical resistance of the MC4217 header was measured at the end of the assembly process to ensure the wire bonds to the SCB and header were successfully connected. Resistance in the range of 1.00 to 1.10 Ohm was typical.

It should be noted that the assembly process for these headers was somewhat exploratory because no wire bond tooling "specific-to-the-task" was used. In addition, the SCB chip was adapted instead of designed to this application. There exists the possibility, under the activities of SCB chip size optimization and the use of adequate wire bond tooling for holding and moving the MC4217 header, that the assembly process could be reduced to a fully operator-independent task.

Furthermore, the use of an optimized SCB chip design should offer several other advantages, such as; the initiator resistance (which is determined by the resistivity of the bridge material), bridge orientation (parallel, perpendicular, or any other direction), and different land metalization (aluminum, gold, tungsten, etc) for powder material compatibility. All these advantages are possible without changing the die size and with minimal modifications to the fabrication process.

2.3 – 6 Subtask 6: Build Retrofitted MC4217 Detonators with CP and BNCP.

The Ensign-Bickford Company (EBCo) completed this work and a short synopsis is presented here. Reference 6 has more information.

Sandia provided twenty-three MC4217 headers to SBCT for replacement of the 0.020" long exploding bridgewire with a modified 3-2B1 SCB. These headers were rejected from the normal MC4217 production activities due to cosmetic reasons only, and were functionally acceptable. The headers provided did not have sleeves attached, which allowed SCB mounting on the Insert.

There were two mounting configurations proposed for the SCB chips, offset and diagonal. Several SCB chips were attached in the offset configuration, as shown in Figure 2-17 which created an interference with the sleeve. It was soon discovered that the diagonal configuration did not pose an interference with the MC4217 sleeve and would be centered at the base of the explosive charge, as seen in Fig. 2-18. Because the

diagonal configuration offered the better design, the offset SCBs were removed from their headers and replaced with diagonal SCBs.

The twenty-three MC4217 Detonators with the "diagonal" SCBs attached were shipped along with BNCP to EBCo in Simsbury Connecticut. The detonators underwent laser welding of the sleeves, pressing of the CP and BNCP powders, loading of the HMX pellet, and laser welding of the closure disk. The procedures were similar to the MC4217 production procedures.

2.3 – 7 Subtask 7: Preliminary Test of MC4217 Detonators with CP and BNCP.

The twenty-three SCB/MC4217 units were returned to Sandia for testing. Six units were separated from the lot to be tested with a Velocity Interferometer System for Any Reflector (VISAR) system to infer the output pressure. Of these six units, three were loaded with CP/HMX and three were loaded with BNCP/HMX. The remaining seventeen units, eight with CP/HMX and nine with BNCP/HMX, were tested with Time of Arrival Detector (TOAD) pins to determine function time.

VISAR Testing

In order to determine output pressure of the SCB MC4217 Detonators, the VISAR system was used. Output pressure is calculated from the measured particle velocity of the interface between the output disk and a reflective coating on a transparent window, as determined by the VISAR. To create the interface, an adapter was manufactured of 3/8" diameter by 1/4" thick PMMA, aluminized at the interface. This assembly was placed over the barrel of the detonator and glued in place such that the window was in contact with the output disk of the detonator.

The results from this VISAR testing are given in Table 2-5. The average CP/HMX peak output velocity was 1.49 mm/μs resulting in a calculated peak pressure of 87.3 kBar. The mean BNCP/HMX output velocity was 1.79 mm/μs resulting in a calculated pressure of 112.5 kbar. A representative particle velocity VISAR trace is given in Fig. 2-19. Oscillations following the initial shock jump are from an impedance mismatch between the steel closure disk and the PMMA window and are expected.

For comparison purposes, three production MC4217 Detonators were tested using the VISAR system to determine output particle velocity. The average production MC4217 particle velocity was 1.60 mm/μs resulting in a calculated pressure of 97.6 kbar. Data from these three tests are given in Table 2-6.

TOAD Testing

The remaining seventeen SCB MC4217 units were tested using TOAD pins to determine output function time. Data from these tests are given in Table 2-7 and Fig. 2-20. The BNCP/HMX loaded detonators had an average function time of 1.552 μs with a standard deviation of 0.049 μs. These units had considerably lower function times and standard

deviations than the CP/HMX loaded detonators. The CP/HMX loaded detonators had an average function time of 3.761 μs with a standard deviation of 0.376 μs.

2.4 - DISCUSSION

From testing, it was observed that SCB initiated CP MC4217 Detonators showed longer function times than the EBW MC4217 Detonators . A possible hypothesis to explain the slower times is because the CP powder used for the EBW detonator was interlocked crystalline agglomerate in the 50 μm to 100 μm range. This CP powder has been designed for hot-wire DDT applications. CP powder has been experimentally proven to perform well in EBW DDT applications but has not been designed for SCB applications. experimental results from Subtask 4 appear to support this fact. The SCB initiated BNCP MC4217 detonators functioned faster than the EBW MC4217 detonator.

However, incorporation of the SCB into the MC4217 using BNCP as the initial load will require, as a minimum, qualification of the BNCP, hostile environment qualification, shock and vibration testing, and thermal cycling of the device to the weapon system's Stockpile to Target Sequence (STS) requirements.

2.5 - CONCLUSIONS

The MC4217 EBW Detonator used in the WR stockpile has a function time specification of 2.03 μs to 2.23 μs with a range within the lot of no greater than 0.120 μs. Experiments demonstrated the SCB version of the MC4217 using CP had a mean function time of 3.761 μs with a range of 1.118 μs. The SCB version of the MC4217 using BNCP had a mean function time of 1.552 μs with a range of 0.116 μs.

The SCB with perpendicular orientation and low density powders (approximately one half the TMD) proved the combination to provide the best function times. For this reason, the perpendicular orientation using the given firing set parameters is the recommended SCB configuration for future experiments.

It was proven that CP and BNCP will DDT with SCB initiation but more work is needed on powder morphology. Optimizing the powder for SCB applications is necessary before the SCB can be incorporated into the MC4217. Judging from experimental data, the BNCP powder looks to be more promising for SCB applications than CP powder.

The MC4217 mounted with an off-the-shelf 3-2B1 SCB can successfully initiate CP and BNCP powders. One limiting factor to optimizing an SCB for the MC4217 Detonator is the 0.019" pin spacing. The standard 3-2B1 SCB is 0.045" wide. The proposed low resistance SCB design would provide both lower resistance and a larger bridge surface area to make contact with the powder. This combination should allow more plasma energy into the powder than the 3-2B1 SCB.

The firing system in use for the MC4217 is designed for an EBW detonator and likely provides a large all-fire margin of safety for the SCB design. Because of the reduced energy requirements for SCB initiation, future firing set volumes and weights could possibly be reduced with the incorporation of SCB devices.

This initial testing has shown that the SCB MC4217, with BNCP powder, provides better function times with comparable standard deviations to the existing EBW MC4217. With further investigation, testing, and design, this SCB variant of the MC4217 has the potential to be considered an improvement to the EBW design.

Logistically, the SCB device has the potential to remove the EBW welding bottleneck in manufacturing. Because wire bonding of the SCB device would likely utilize a significantly easier process, specially trained personnel would not be required. With this backup in manufacturing eliminated, cost and schedule constraints could be greatly improved.

In addition, the SCB detonator promises to establish a new product for Ensign Bickford Co. Currently, there are a number of manufacturers of EBW detonators, all competing in a very tight explosives market. An SCB detonator has the potential to create an entirely new product with significant advantages over EBW devices.

Finally, the goal of this work was to provide a reliable, fieldable, and cost effective SCB MC4217 with which the change will be nearly transparent to the system the end user. Clearly, there is still work to do in the areas of SCB chip optimization, explosive powder density and morphology, and reliability to meet tactical requirements. We feel confident that these challenges are achievable.

2.6 - ACKNOWLEDGEMENTS

We would like to thank the following for their support and many useful discussions during the completion of this project: Robert Bickes Jr., William Brigham, Steve Harris, Tom Massis, William Tarbell, David Wackerbarth, (all Sandia National Laboratories).

2.7 - REFERENCES

1. D. A. Benson, M. E. Larsen, A. M. Redlund, W. M. Trott, and R. W. Bickes Jr., *Semiconductor Bridge: A Plasma Generator for the Ignition of Explosives,* Journal of Applied Physics, 62 (5), 1 September 1987.

2. SCB Technologies, Inc., Bernardo Martinez-Tovar, Technical Manager, 1009 Bradbury Dr. SE, Albuquerque, NM 87106, Ph: (505) 272-7573, Fax: (505) 272-7568

3. R. W. Bickes Jr., *Smart Semiconductor Bridge (SCB) Igniter for Explosives,* Paper No. 2, 3rd Canadian Symposium on Mining Automation, September 14, 15, 16, 1988.

4. A. P. Montoya, M. L. Reichenbach, *Explosive-Powder Compaction System,* SAND80-1872, Sandia National Laboratories, Albuquerque, NM, September 1981.

5. Presentation by Pacific Scientific Energy Dynamics Division, "CP and BNCP, A Suitable Replacement for Primary Explosives".

6. Ensign-Bickford Company, Tom Beckman, 660 Hopmeadow Street, Simsbury, CT, 06070, Ph: (860) 843-2058.

(THIS PAGE INTENTIONALLY LEFT BLANK)

2.8 FIGURES

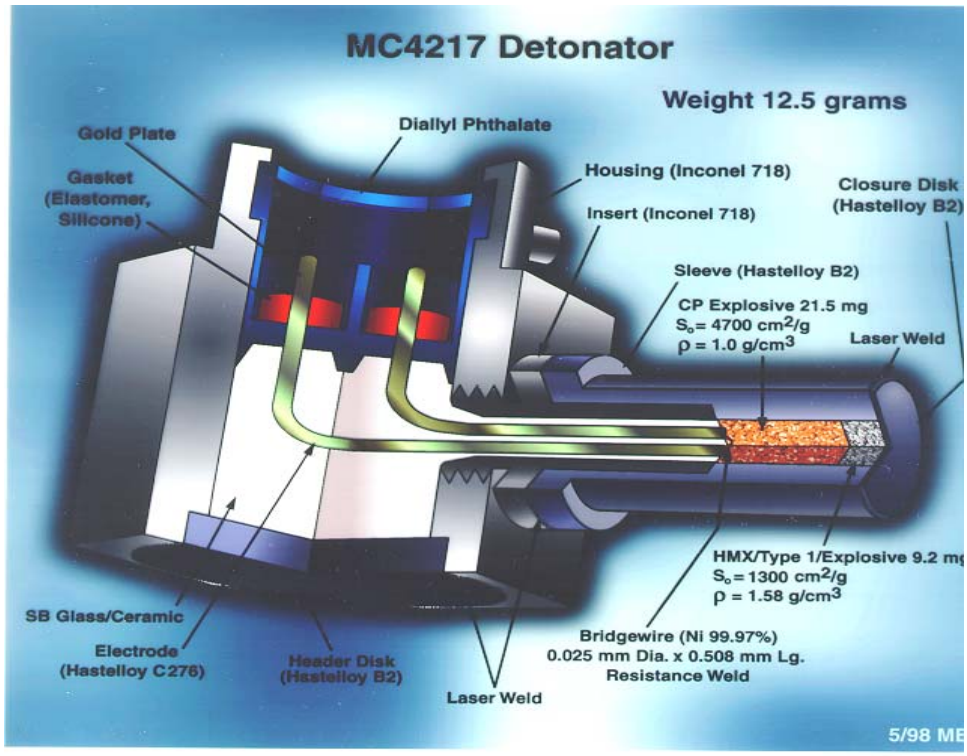

Figure 2- 1. Cutaway of the MC4217 Detonator.

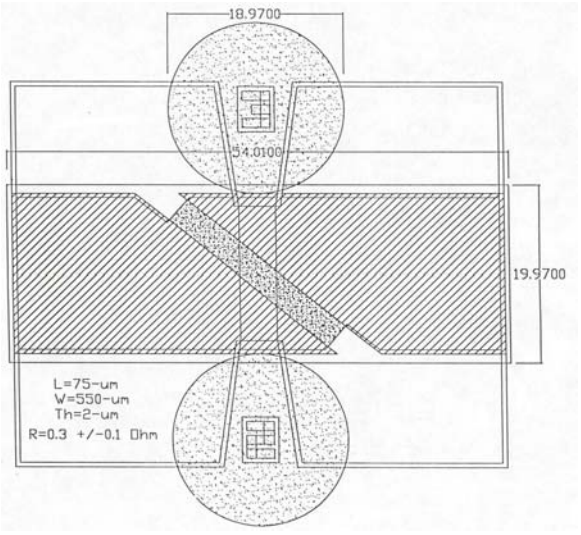

Figure 2- 2. Proposed Low Resistance (0.3 Ohm) SCB to Fit Between the MC4217 Pins.

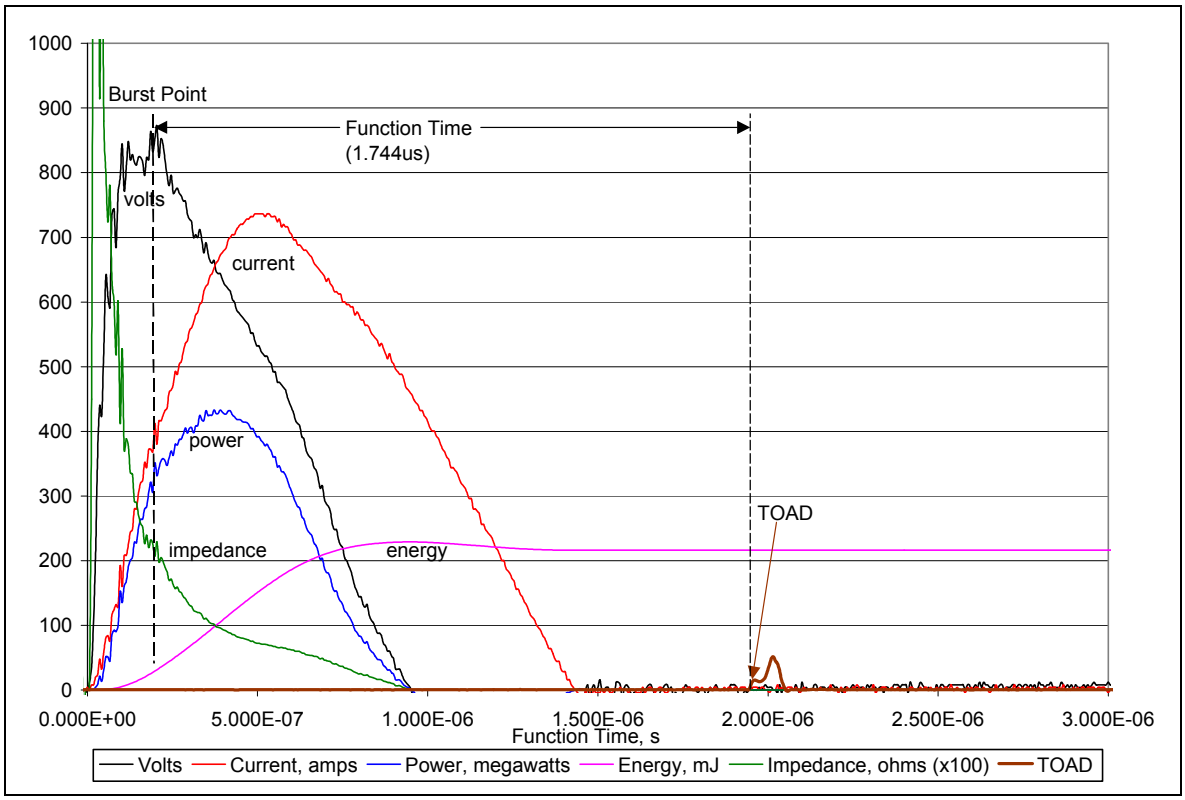

Figure 2- 3. Output Data from Functioning the Low Resistance (0.75 Ohm) SCB.

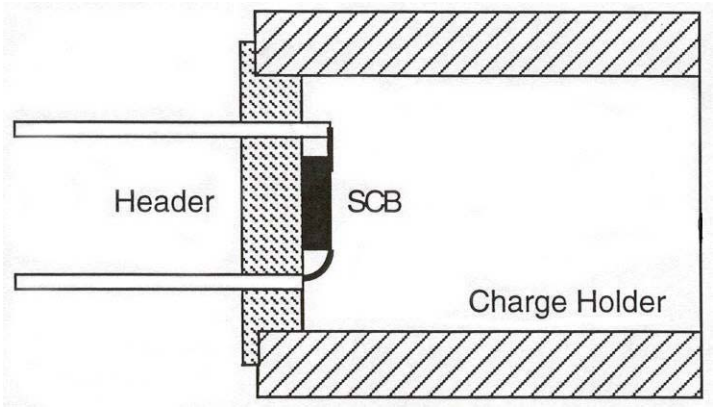

Figure 2- 4. TO46 Header (transistor base) with SCB and brass charge holder.

Figure 2- 5. Photograph of CRADA test hardware.

Figure 2- 6. TO46 Header with 3-2B1 SCB Mounted in Perpendicular Orientation.

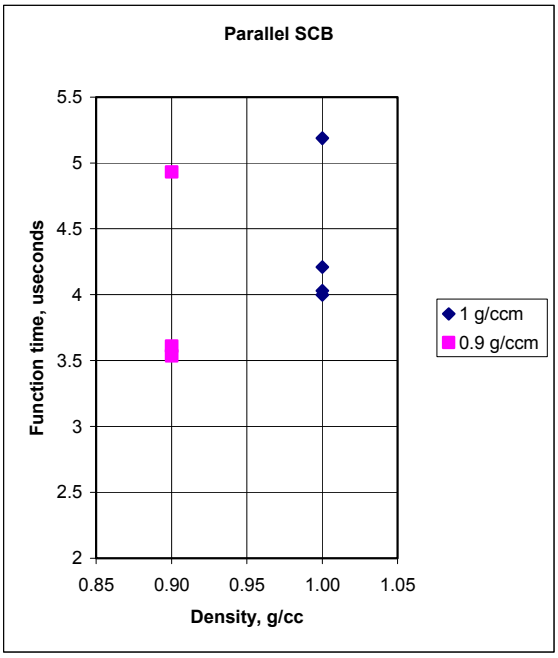

Figure 2- 7. Parallel Orientation.

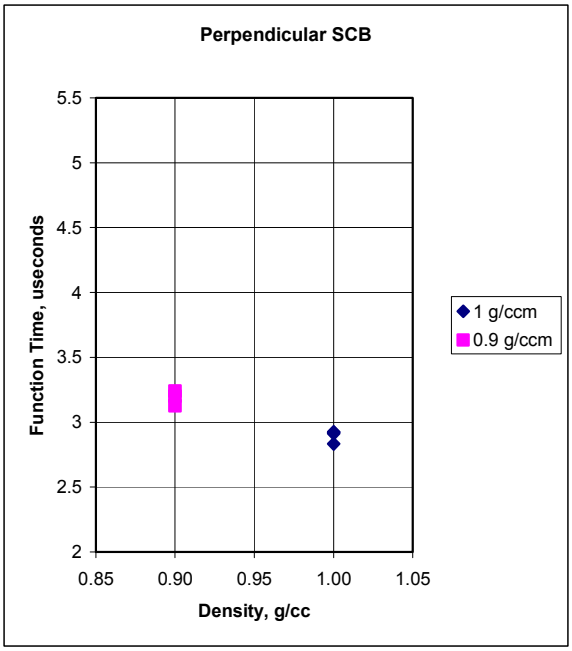

Figure 2- 8. Perpendicular Orientation

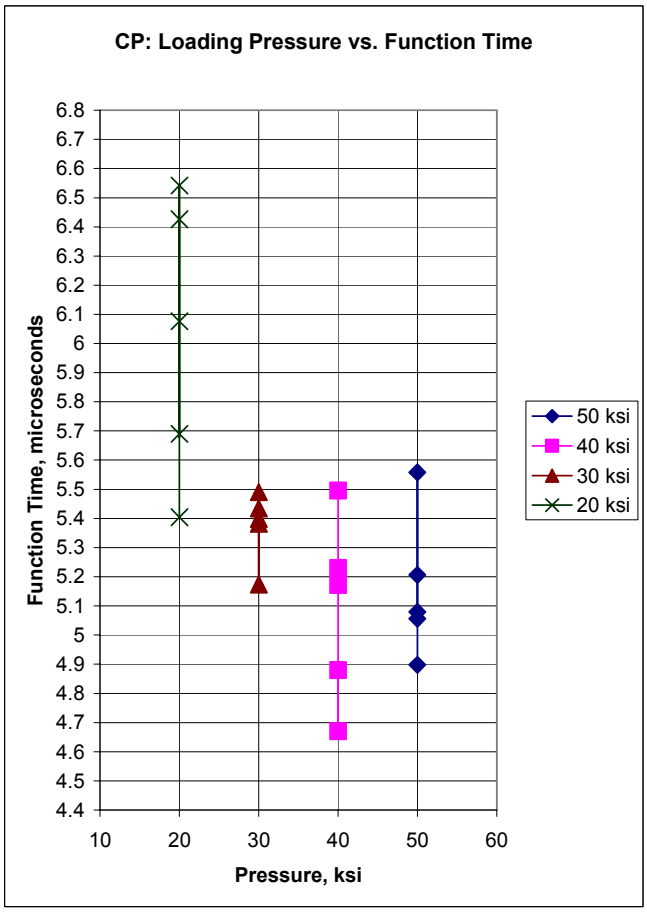

Figure 2- 9. Initial Density Study Results.

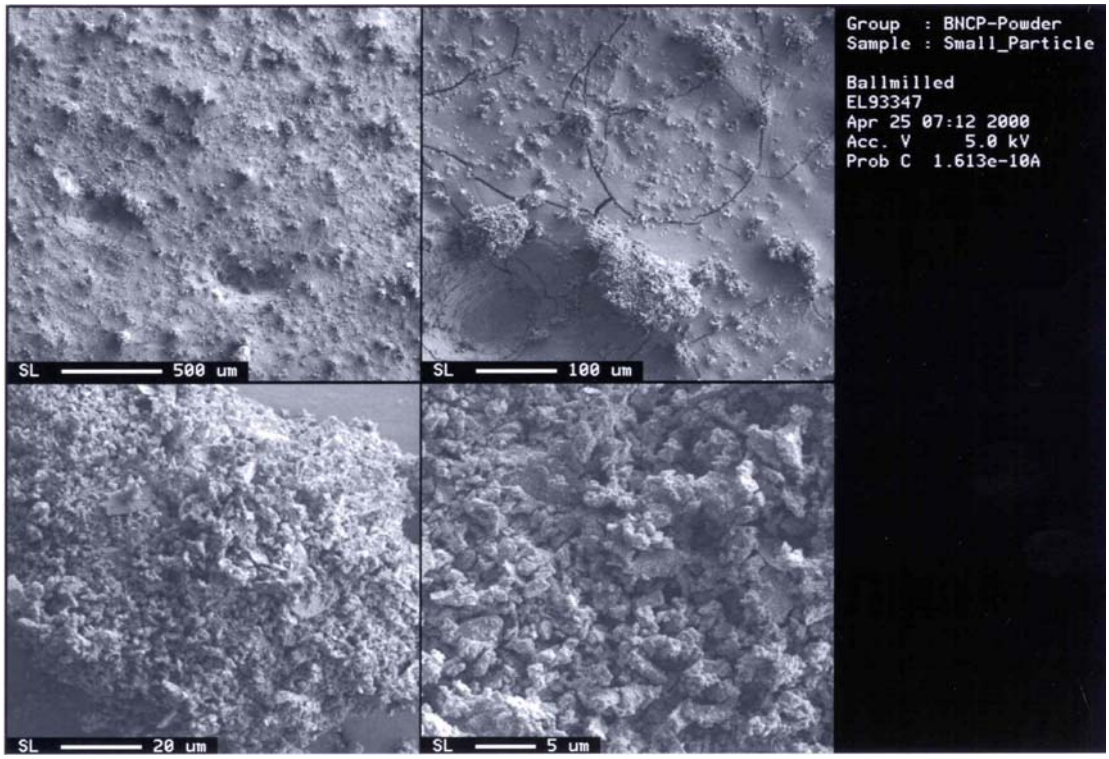

Figure 2- 10. SEM of 2 micron BNCP.

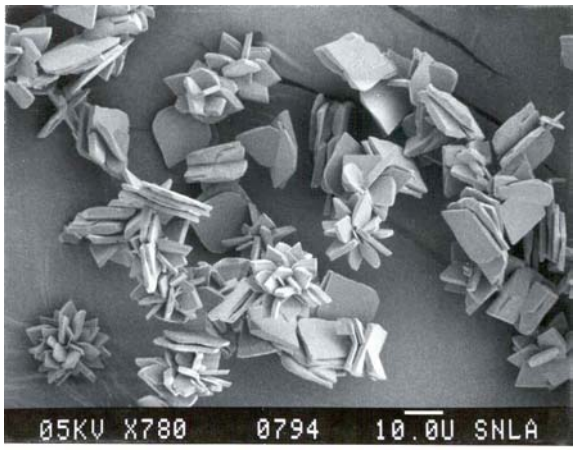

Figure 2- 11. SEM of 20 micron BNCP, 780x.

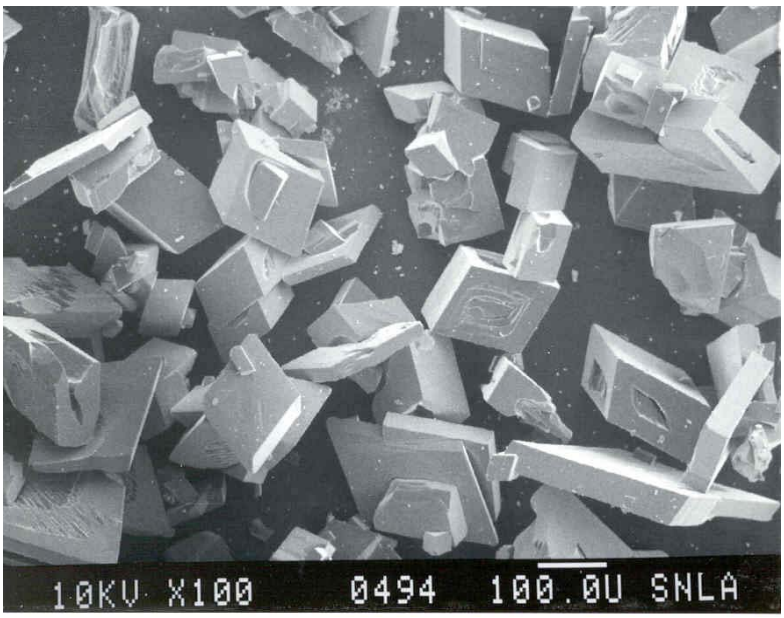

Figure 2- 12. SEM of 20 micron BNCP, 100x

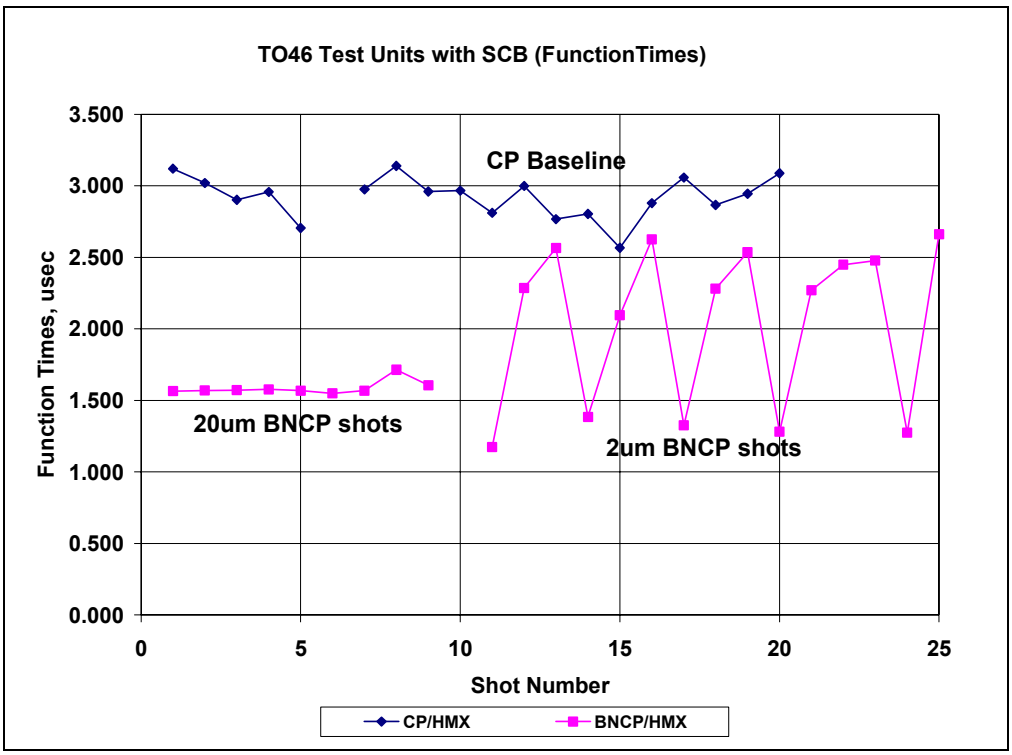

Figure 2- 13. CP/HMX and BNCP/HMX Test Results.

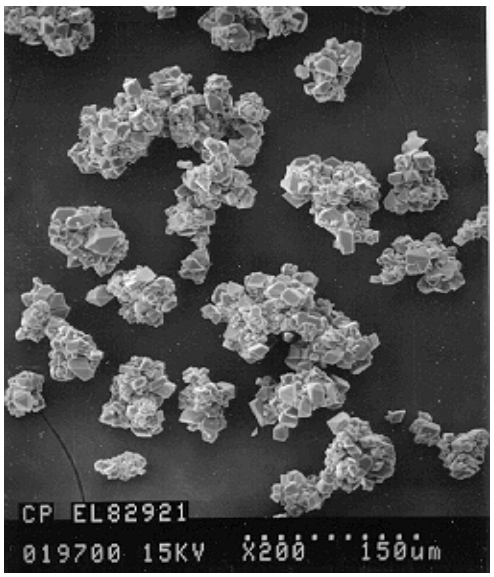

Figure 2- 14. SEM of CP Powder, 200x.

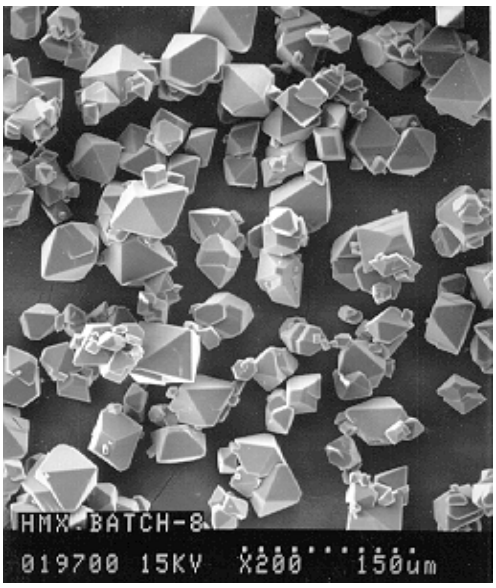

Figure 2- 15. SEM of HMX Powder, 200x.

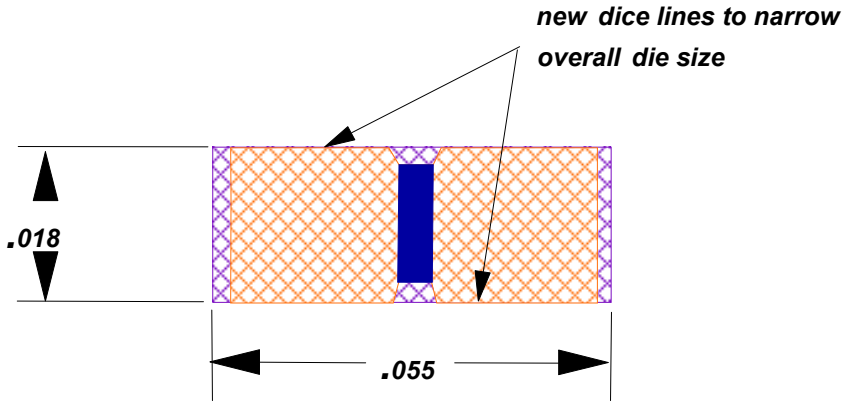

Figure 2- 16. Modified 3-2B1 SCB to fit Between the MC4217 Pins.

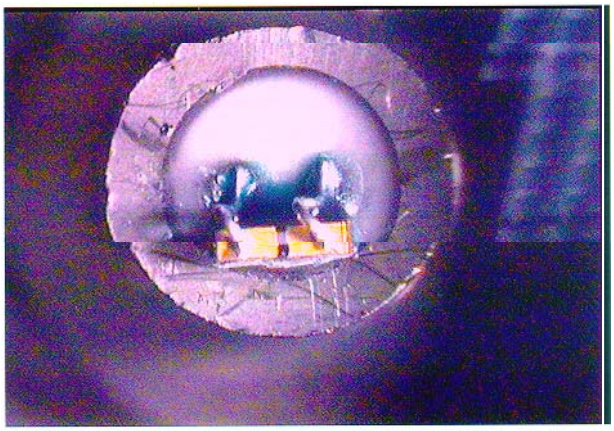

Figure 2- 17. Offset Configuration of the SCB on the MC4217 Detonator. The SCB chip is glued to the SB glass insulator and 5-mil wires are bonded to the chip and the metal pins in the header.

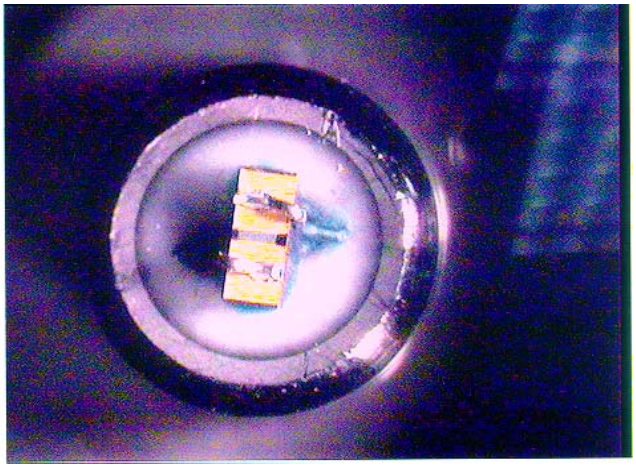

Figure 2- 18. Diagonal Configuration of the SCB on the MC4217 Detonator.

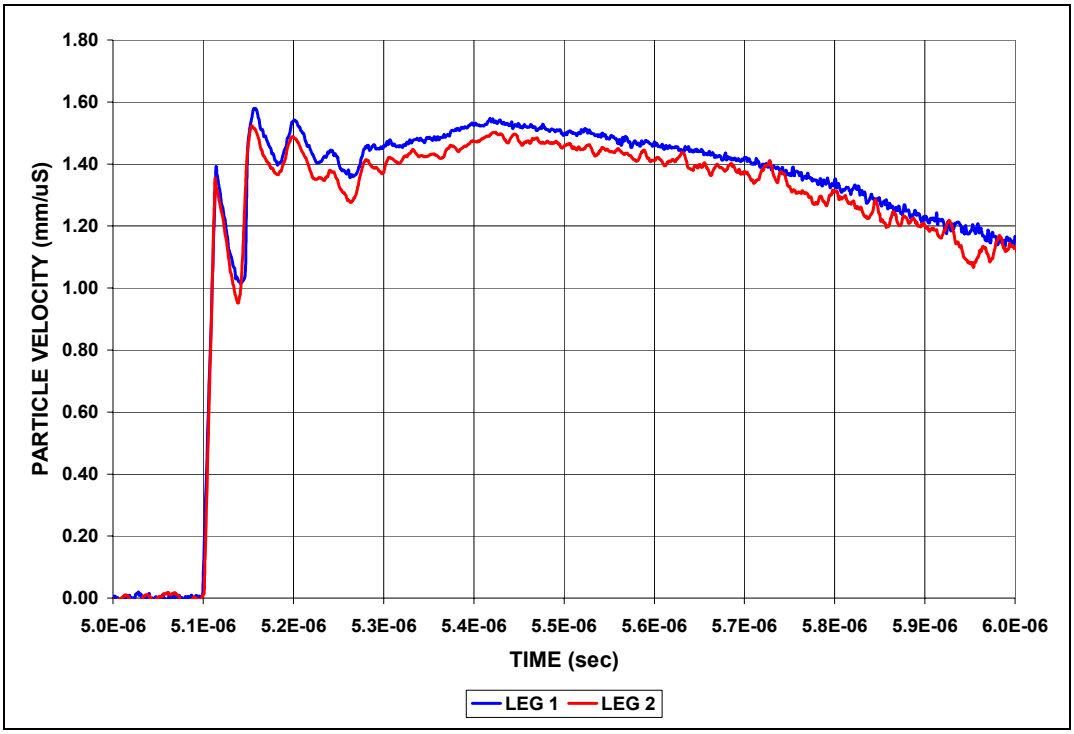

Figure 2- 19. VISAR data of CP loaded MC4217 Detonator with SCB.

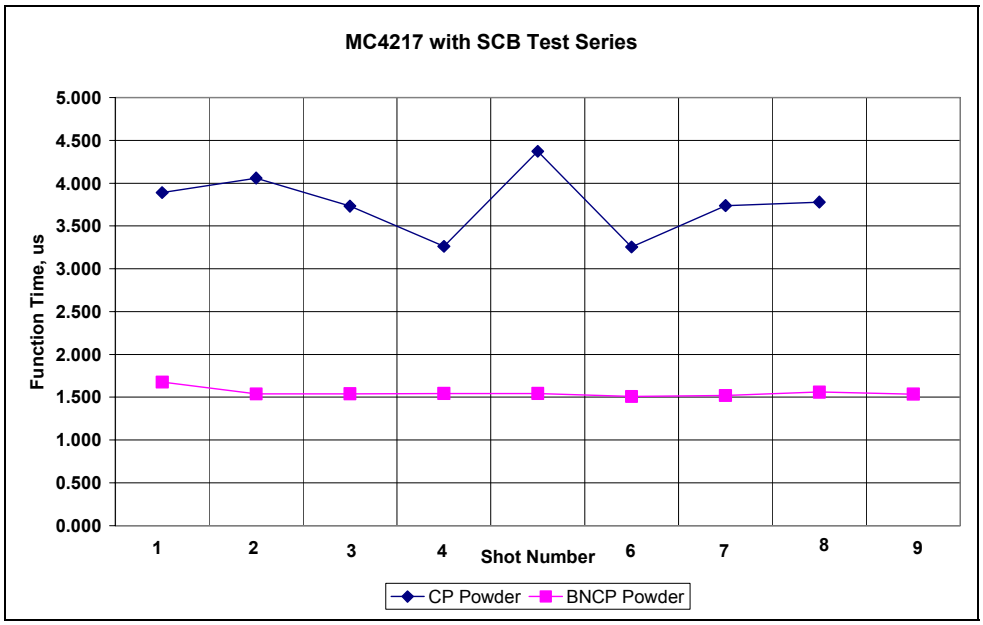

Figure 2- 20. Traces of CP and BNCP loaded SCB MC4217 Detonator Function Times.

2.9 TABLES

Table 2- 1. CRADA 98/1540 Task 1 Subtasks

Task No.	Subtask No.	Task Description	Duration (Month of CRADA)	Responsible Parties
I		**MC4217 Retrofit**	**01-24**	**SANDIA/EBCo**
	1	Design of a low resistance die.	01-03	SANDIA/EBCo
	2	Preliminary design review of SCB insertion requirements	02	SANDIA/EBCo
	3	Process 3-2B1 and low resistance die and mount on T046 headers	04-06	SCBT
	4	Characterize and test SCB die on T046 headers	07-09	SANDIA
	5	Develop bonding process to attach SCBs into MC4217 detonators	10-12	SCBT
	6	Build retrofitted MC4217 detonators with CP and BNCP	13-16	EBCo.
	7	Preliminary test of MC4217 units	17-19	SANDIA
	8	Summary Reports	23-24	EBCo/SANDIA

Table 2- 2. Parallel and Perpendicular SCB Functioning

SCB Type	Test Fixture	Fire Set	Orientation	Powder	Mass, mg	Density, g/cc	# Tests	Mean Timing μs	StDev μs
3-2B1	TO46/Brass	TC1061	Parallel	CP	77.0	1.00	4	**4.356**	**0.562**
3-2B1	TO46/Brass	TC1061	Parallel	CP	69.0	0.90	3	**4.026**	**0.786**
3-2B1	TO46/Brass	TC1061	Parallel	CP	127.0	1.66	1	**6.475**	**N/A**
3-2B1	TO46/Brass	TC1061	Perpendicular	CP	77.0	1.00	4	**2.898**	**0.044**
3-2B1	TO46/Brass	TC1061	Perpendicular	CP	69.0	0.90	3	**3.189**	**0.058**
3-2B1	TO46/Brass	TC1061	Perpendicular	CP	127.0	1.66	1	**6.710**	**N/A**

Table 2- 3. Initial CP Density Study Results

Pressure ksi	Density g/cc	Force on Ram lbs	# Tests	Mean Timing μs	Standard Deviation μs	Range μs
50	1.96	883	5	5.160	0.248	1.138
40	1.86	707	5	5.090	0.321	0.826
30	1.66	530	5	5.376	0.120	0.316
20	1.58	353	5	6.028	0.482	0.514

Table 2- 4. CP/HMX and BNCP/HMX Configurations

Powder	Mass, mg	Density, g/cc	Powder	Mass, mg	Density, g/cc	# Tests	Avg	STD	Min	Max	Range
CP	52.2	1.00	HMX	23.00	1.58	19	2.922	0.146	2.566	3.139	0.573
BNCP, 20micron	52.2	1.00	HMX	23.00	1.58	9	1.587	0.050	1.550	1.714	0.164
BNCP, 2micron	52.2	1.00	HMX	23.00	1.58	15	2.045	0.575	1.175	2.660	1.485

Table 2- 5. VISAR Testing with SCB mounted MC4217

UNIT SERIAL NUMBER	TYPE EXPLOSIVE	PARTICLE VELOCITY (mm/μs)	PRESSURE INTO PMMA (kbar)
010	CP/HMX	1.65	99.8
007	CP/HMX	1.45	82.5
004	CP/HMX	1.38	79.8
013	BNCP/HMX	1.70	104.3
015	BNCP/HMX	1.87	120.5
014	BNCP/HMX	1.79	112.8

Table 2- 6. VISAR Testing with Production MC4217

UNIT SERIAL NUMBER	TYPE EXPLOSIVE	PARTICLE VELOCITY (mm/μs)	PRESSURE INTO PMMA (kbar)
4961	CP/HMX	1.62	97.1
4964	CP/HMX	1.66	106.6
4997	CP/HMX	1.53	89.2

Table 2- 7. SCB mounted into MC4217 detonator function timing.

SCB Orientation	Explosive Train	# Tests	Avg. Timing (μs)	STD (μs)	Max (μs)	Min (μs)	Range (μs)
Perpendicular	CP/HMX	8	3.761	0.376	4.372	3.254	1.118
Perpendicular	BNCP/HMX	9	1.552	0.049	1.676	1.510	0.116

2.10 APPENDIX A

CP Density Study Summary

1. The technician pressed five each TO46 headers at four different CP densities. The units were pressed to 50 kpsi, 40 kpsi, 30 kpsi, and 20 kpsi. The amount of explosive in each unit was weighed after pressing. The powder was skimmed flush to the top of each charge holder. The allocation of TO46 headers follow:

a. 5 headers pressed at 50 kpsi.
b. 5 headers pressed at 40 kpsi.
c. 5 headers pressed at 30 kpsi.
d. 5 headers pressed at 20 kpsi.

2. The technician weighed the amount of powder pressed for each header. The mean weights follow:
   a. 5 headers with 150 mg of CP
   b. 5 headers with 142 mg of CP
   c. 5 headers with 127 mg of CP
   d. 5 headers with 121 mg of CP

3. The internal volume of the TO46 header with charge holder is 0.00473 in^3. The volume of the SCB is 0.000054 in^3. The net volume available for powder loading was 0.00467 in^3 or 0.07653 cm^3. Given the measured weight of CP pressed at each pressure the densities calculate to be:
   a. 1.96 g/cm^3
   b. 1.86 g/cm^3
   c. 1.66 g/cm^3
   d. 1.58 g/cm^3

4. A PMMA cap that held the Time of Arrival Detector (TOAD) was placed on top of the charge holder. The PMMA cap was glued in place. The TOAD was installed. Function time data was collected for each density. A curve relating density to function time was generated.

2.11 APPENDIX B

Table 2- 8. Parallel and Perpendicular SCB Functioning

SCB Type	Test Fixture	Firing Set	Orientation	Powder	Mass, mg	Density, g/cc	Shot #	Function Time, μs
3-2B1	TO46/Brass	TC1061	Parallel	CP	77.0	1.00	1714	4.029
3-2B1	TO46/Brass	TC1061	Parallel	CP	77.0	1.00	1718	5.187
3-2B1	TO46/Brass	TC1061	Parallel	CP	77.0	1.00	1719	3.999
3-2B1	TO46/Brass	TC1061	Parallel	CP	77.0	1.00	1721	4.210
							Mean	**4.356**
							SDEV	**0.562**
3-2B1	TO46/Brass	TC1062	Parallel	CP	69.0	0.90	1722	3.536
3-2B1	TO46/Brass	TC1063	Parallel	CP	69.0	0.90	1723	4.932
3-2B1	TO46/Brass	TC1064	Parallel	CP	69.0	0.90	1724	3.609
							Mean	**4.026**
							SDEV	**0.786**
3-2B1	TO46/Brass	TC1062	Parallel	CP	127.0	1.66	1712	6.475
3-2B1	TO46/Brass	TC1061	Perpendicular	CP	77.0	1.00	1713	2.832
3-2B1	TO46/Brass	TC1061	Perpendicular	CP	77.0	1.00	1716	2.923
3-2B1	TO46/Brass	TC1061	Perpendicular	CP	77.0	1.00	1717	2.925
3-2B1	TO46/Brass	TC1061	Perpendicular	CP	77.0	1.00	1720	2.911
							Mean	**2.898**
							SDEV	**0.044**
3-2B1	TO46/Brass	TC1061	Perpendicular	CP	69.0	0.90	1725	3.126
3-2B1	TO46/Brass	TC1061	Perpendicular	CP	69.0	0.90	1726	3.239
3-2B1	TO46/Brass	TC1061	Perpendicular	CP	69.0	0.90	1727	3.201
							Mean	**3.189**
							SDEV	**0.058**
3-2B1	TO46/Brass	TC1061	Perpendicular	CP	127.0	1.66	1711	6.710

Table 2- 9. Initial CP Density Study Results

Pressure ksi	Density G/cc	Force on Ram lbs.	Shot #	Function Time, μs
50	1.96	883	1	4.898
50	1.96	883	2	5.206
50	1.96	883	3	5.558
50	1.96	883	4	5.056
50	1.96	883	5	5.080
			Mean	5.160
			SDEV	0.248
			Range	1.138
40	1.86	707	1	4.880
40	1.86	707	2	4.670
40	1.86	707	3	5.230
40	1.86	707	4	5.172
40	1.86	707	5	5.496
			Mean	5.090
			SDEV	0.321
			Range	0.826
30	1.66	530	1	5.434
30	1.66	530	2	5.382
30	1.66	530	3	5.398
30	1.66	530	4	5.174
30	1.66	530	5	5.490
			Mean	5.376
			SDEV	0.120
			Range	0.316
20	1.58	353	1	5.404
20	1.58	353	2	6.542
20	1.58	353	3	5.690
20	1.58	353	4	6.076
20	1.58	353	5	6.426
			Mean	6.028
			SDEV	0.482
			Range	0.514

Table 2- 10. Test Data of CP/HMX and BNCP/HMX configurations.

Powder	Mass, mg	Density, g/cc	Powder	Mass, mg	Density, g/cc	Shot #	Function Time, μs
			Pellet				
CP	52.2	1.00	HMX	23.00	1.58	1737	3.120
CP	52.2	1.00	HMX	23.00	1.58	1738	3.020
CP	52.2	1.00	HMX	23.00	1.58	1739	2.902
CP	52.2	1.00	HMX	23.00	1.58	1740	2.957
CP	52.2	1.00	HMX	23.00	1.58	1741	2.705
CP	52.2	1.00	HMX	23.00	1.58	1743	2.975
CP	52.2	1.00	HMX	23.00	1.58	1744	3.139
CP	52.2	1.00	HMX	23.00	1.58	1745	2.960
CP	52.2	1.00	HMX	23.00	1.58	1746	2.966
CP	52.2	1.00	HMX	23.00	1.58	1747	2.811
CP	52.2	1.00	HMX	23.00	1.58	1748	2.999
CP	52.2	1.00	HMX	23.00	1.58	1749	2.767
CP	52.2	1.00	HMX	23.00	1.58	1750	2.803
CP	52.2	1.00	HMX	23.00	1.58	1751	2.566
CP	52.2	1.00	HMX	23.00	1.58	1752	2.878
CP	52.2	1.00	HMX	23.00	1.58	1753	3.058
CP	52.2	1.00	HMX	23.00	1.58	1754	2.866
CP	52.2	1.00	HMX	23.00	1.58	1755	2.944
CP	52.2	1.00	HMX	23.00	1.58	1756	3.087
						Avg	**2.922**
						STD	**0.146**
						Max	**3.139**
						Min	**2.566**
						Range	**0.573**
BNCP, 20micron	52.2	1.00	HMX	23.00	1.58	1757	1.564
BNCP, 20micron	52.2	1.00	HMX	23.00	1.58	1758	1.569
BNCP, 20micron	52.2	1.00	HMX	23.00	1.58	1759	1.571
BNCP, 20micron	52.2	1.00	HMX	23.00	1.58	1760	1.577
BNCP, 20micron	52.2	1.00	HMX	23.00	1.58	1761	1.568
BNCP, 20micron	52.2	1.00	HMX	23.00	1.58	1762	1.550
BNCP, 20micron	52.2	1.00	HMX	23.00	1.58	1763	1.568
BNCP, 20micron	52.2	1.00	HMX	23.00	1.58	1764	1.714
BNCP, 20micron	52.2	1.00	HMX	23.00	1.58	1765	1.606
						Avg	**1.587**
						STD	**0.050**
						Max	**1.714**
						Min	**1.550**
						Range	**0.164**
BNCP, 2micron	52.2	1.00	HMX	23.00	1.58	1767	1.175
BNCP, 2micron	52.2	1.00	HMX	23.00	1.58	1768	2.286
BNCP, 2micron	52.2	1.00	HMX	23.00	1.58	1769	2.564
BNCP, 2micron	52.2	1.00	HMX	23.00	1.58	1770	1.385
BNCP, 2micron	52.2	1.00	HMX	23.00	1.58	1771	2.095
BNCP, 2micron	52.2	1.00	HMX	23.00	1.58	1772	2.626
BNCP, 2micron	52.2	1.00	HMX	23.00	1.58	1773	1.326
BNCP, 2micron	52.2	1.00	HMX	23.00	1.58	1774	2.280
BNCP, 2micron	52.2	1.00	HMX	23.00	1.58	1775	2.535
BNCP, 2micron	52.2	1.00	HMX	23.00	1.58	1776	1.281
BNCP, 2micron	52.2	1.00	HMX	23.00	1.58	1777	2.269
BNCP, 2micron	52.2	1.00	HMX	23.00	1.58	1778	2.448
BNCP, 2micron	52.2	1.00	HMX	23.00	1.58	1779	2.477
BNCP, 2micron	52.2	1.00	HMX	23.00	1.58	1780	1.274
BNCP, 2micron	52.2	1.00	HMX	23.00	1.58	1781	2.660
						Avg	**2.045**
						STD	**0.575**
						Max	**2.660**
						Min	**1.175**
						Range	**1.485**

Table 2- 11. SCB mounted into MC4217 detonator function times.

SCB Orientation	Powder	Mass, mg	Density, g/cc	Powder Pellet	Mass, mg	Density, g/cc	Shot #	Function Time, μs
Perpendicular	CP	21.5	1.00	HMX	9.20	1.58	1802	3.890
Perpendicular	CP	21.5	1.00	HMX	9.20	1.58	1803	4.060
Perpendicular	CP	21.5	1.00	HMX	9.20	1.58	1804	3.732
Perpendicular	CP	21.5	1.00	HMX	9.20	1.58	1805	3.262
Perpendicular	CP	21.5	1.00	HMX	9.20	1.58	1806	4.372
Perpendicular	CP	21.5	1.00	HMX	9.20	1.58	1807	3.254
Perpendicular	CP	21.5	1.00	HMX	9.20	1.58	1808	3.738
Perpendicular	CP	21.5	1.00	HMX	9.20	1.58	1809	3.780
							Avg	**3.761**
							STD	**0.376**
							Max	**4.372**
							Min	**3.254**
							Range	**1.118**
Perpendicular	BNCP	21.5	1.00	HMX	9.20	1.58	1810	1.676
Perpendicular	BNCP	21.5	1.00	HMX	9.20	1.58	1811	1.538
Perpendicular	BNCP	21.5	1.00	HMX	9.20	1.58	1812	1.540
Perpendicular	BNCP	21.5	1.00	HMX	9.20	1.58	1813	1.544
Perpendicular	BNCP	21.5	1.00	HMX	9.20	1.58	1814	1.544
Perpendicular	BNCP	21.5	1.00	HMX	9.20	1.58	1815	1.510
Perpendicular	BNCP	21.5	1.00	HMX	9.20	1.58	1816	1.520
Perpendicular	BNCP	21.5	1.00	HMX	9.20	1.58	1817	1.560
Perpendicular	BNCP	21.5	1.00	HMX	9.20	1.58	1818	1.536
							Avg	**1.552**
							STD	**0.049**
							Max	**1.676**
							Min	**1.510**
							Range	**0.116**

(THIS PAGE INTENTIONALLY LEFT BLANK)

3.0 Task 2: Visible Emission from a Semiconductor Bridge Interface With an Ignited Energetic Material

Anita M. Renlund and Jill C. Miller
Sandia National Laboratories
P.O. Box 5800
Albuquerque, NM 87185-1454

ABSTRACT

We monitored the visible emission from a semiconductor bridge (SCB) ignitor in contact with pressed energetic materials. The SCBs were fabricated from doped polysilicon on sapphire substrates, then mounted on plastic headers with a through-hole for monitoring emission from the backside of the bridge. The header was attached to a metal sleeve and energetic material (EM) powder was pressed against the SCB. Different EMs were studied, including THKP (Titanium subhydride potassium perchlorate), CP(1-(5-cyanotretrazolato)pentaamine cobalt(III) perchlorate), BNCP (2-(5-nitro-tetrazolato)tetramine cobalt(III) perchlorate), and ZPP (Zirconium potassium perchlorate). Gated emission spectra from 300-600 nm were obtained at different delays from the onset of SCB plasma formation, and we observed qualities of the spectra associated with electronic energy transfer from the plasma to heavy metals in some of the EM powders.

3-1 INTRODUCTION

This report summarizes work completed under task 2 of the CRADA. The semiconductor bridge (SCB) is a Sandia patented technology licensed by EBCo, a supplier of components to Sandia and a manufacturer of commercial explosive devices. This task was specifically aimed at investigating the initiation mechanism of energetic materials (EMs) by low-voltage SCB igniters[1] to elucidate any possible role of electronic energy transfer from the ignition plasma to EMs. Modeling of explosive components is difficult because details of the initiation process are not well known. The SCB provides a unique opportunity because it can be fabricated on various substrates, including sapphire that can act as an optical window allowing spectroscopic access to the ignition event. Electronic energy transfer from the plasma to the EM is most probable in those EMs that contain heavy metals that may be able to absorb optical energy from the plasma. This mechanism is enhanced if there is sufficient overlap of electronic bands between the emission of the plasma and the absorption spectrum of the EM. The materials selected for this study were CP (1-(5-cyanotretrazolato)pentaamine cobalt(III) perchlorate),

BNCP (2-(5-nitro-tetrazolato)tetramine cobalt(III) perchlorate), Titanium sub-hydride potassium perchlorate, (THKP), and zirconium potassium percholrate (ZPP).

3-2 EXPERIMENTAL

A schematic of the experimental arrangement is shown in Fig. 3-1. Briefly, SCB devices with EM charge holders were fired in an explosive chamber. Light from the SCB plasma or ignited EM was transmitted to a spectrometer using an optical fiber. Emission dispersed through a spectrometer and recorded on an intensified CCD camera. The intensifier was gated on at different times relative to the fire pulse to the SCB in order to obtain indication of reaction progress.

3.2-1 Test Devices

Two different SCB devices were tested. Both were polysilicon on sapphire, but one was a Type 3–2B1A (100 μm x 380 μm, 1-Ohm resistance), and the other a Type 70A2A device (200 μm x 200 μm, 2- Ohm resistance). Most tests were done using the 70A2A bridges because they were available when our work began. Sapphire substrates were needed to allow optical access to the ignition event. SCBs were mounted on headers through which a hole had been drilled . During the assembly process, some of the bridges shifted position, so we did not always have adequate light access. We evaluated the positioning of the bridges on the header by backlighting the header, as shown in Fig. 3-2, prior to loading the powder onto the header. The resistance of each bridge was measured both before and after loading, and any devices where the resistance changed appreciably were not tested. Loading of the EM powders was done at SNL, with the exception of the ZPP devices which were loaded at EBCo. Loading pressures were in the10-20,000 psi range, and charge sizes were between 50 and 100 mg.

3.2-2 Firing System

The SCB devices were fired with a capacitor discharge unit (CDU) firing set. A 20 μF capacitor charged to up to 50 V provided the energy to the bridge. We recorded both bridge voltage and current on each shot. Representative traces are shown in Fig. 3-3. From such traces it is easy to determine whether or not the SCB functioned properly and the time of the plasma formation. The firing pulse provided a quick-rising voltage across the SCB, subsequent heating of the bridge led to reduced resistance and increasing current until the plasma formed, at a time indicated by the dashed vertical line in Fig.3-3. In nearly all cases, the resulting plasma ignited the EM, the only exceptions being some THKP charges.

3.2 -3 Optical and Spectroscopy Systems

The goal of these experiments was to investigate the ignition face of the EM, i.e., the contact face between the SCB and the EM powder. The sapphire substrate effectively blocks transmission of light below about 300 nm. We used an optical fiber inserted through the header to contact the sapphire substrate of the SCB (see Fig. 3-4). Initially the silicon of the SCB blocks any optical access to the powder, but after the plasma is formed the sapphire acts as a window. Fused silica optical fibers of 400 to 800 μm diameters were used to transmit the light from the SCB device, through the port from the explosive chamber, to the input of a 0.5-m spectrometer. An additional optical fiber was usually used to transmit light from the front face of the explosive charge to be used as an additional timing indicator. The current waveform clearly indicated the start of plasma formation, the light from the output end of the charge indicated when the explosive event was completed. We wished to investigate the growth of the explosion from the ignition face at times between these two extremes. Light dispersed by the spectrometer was imaged using a lens-coupled intensifier onto the face of a 1-inch long CCD camera with 1154 by 256 pixel resolution. The intensifier was gated on for a maximum of 2.5 μs, and the delay time was varied from shot to shot to cover the ignition times. Wavelength calibration of the spectrometer was accomplished using standard mercury or neon lamps. Some of the spectra were corrected for the wavelength-dependent response of the system. Those corrections were achieved by obtaining the spectra of a calibrated black-body emitter (quartz-halogen lamp) at 3200 K. These corrected spectra serve primarily to understand the nature of the background emission, but do not address the central investigation of electronic energy transfer.

3.3 - RESULTS AND DISCUSSION

3.3-1 CP

Figures 3-5 and 3-6 show selected spectra obtained during the ignition of CP. This was the only material for which we examined both the Type 3–2B1A and the Type 70A2A SCBs. Each figure contains a "history" of the ignition event, with a spectrum of the plasma only and then spectra early and late in the ignition. Both types of SCBs ignited the CP and we measured repeatable function times near 15 μs, as measured from the intense emission at the output face. The spectral ranges are not exactly the same in the two tests, but the regions of interest are covered in each. The most noticeable difference is the shape of the broad-band emission at late times. The "late" spectrum in the 3–2B1A SCB ignition actually represents a more complete reaction and was later, relative to the plasma formation, than in the other case. The difference is likely of minor significance.

In both cases there is significant attenuation of the strong 396-nm line observed in the plasma spectrum. This is tentatively identified as an Al emission line. Aluminum lands form the contact points for the electrical connections and help define the SCB

dimensions, and intense emission from the Al was previously seen to be formed during the late part of the plasma emission.[1] We did not observe any new emission lines in the early or late spectra from the emission. This does not rule out the possibility of electronic energy transfer to the CP. The emission spectrum of CP has not been well characterized, but there are lines in the ultraviolet below the cut-off of the sapphire transmission.[2]

BNCP

Spectra similar to those presented for CP are shown in Fig. 3-7 for SCB ignition of BNCP. The ignition time of the BNCP was more variable than for CP, so it was difficult to time the 2.5-ms gate to the appropriate part of the ignition pulse. The "early" spectrum in Fig. 3-7 is actually representative of the early heating of the SCB and precedes the plasma formation. The "late" spectrum is similar in time, relative to ignition, to the "early" spectra shown in Figs. 5 and 6. Like the CP, there was significant attenuation of the strong 396-nm plasma line. But unlike the CP, a clear difference in the emission spectrum was observed with additional emission lines. The new emission occurs in a spectral region where emission from BNCP in solution has been observed.[2] The most likely explanation of this new emission is that the BNCP was electronically excited, presumably from absorption of optical energy from the plasma.

ZPP

Devices containing ZPP were tested similar to those described above. Function times were later, typically between 30 and 40 μs. Timing the detector gate to the event was therefore also more difficult. We shot 23 devices and could only obtain one (labeled "Early" in Fig. 3-8, below) that included new emission lines from Zr. The lines are tentatively assigned as the 355- and 360-nm lines from the neutral Zr.[3] Poor signal-to-noise makes other assignments difficult. We did not try to look for K emission near 770 nm.

The ZPP functioned later than the CP and BNCP devices, which was not unexpected for the pyrotehcnic mix. The damage to the fixture was also considerably less, as shown in Fig. 3-9. ZPP is a strong gas generator and did not deform the charge holder to the same extent as the high explosives CP and BNCP.

THKP

Function times for the SCB-firing of THKP in these tests was in the range of 70 –100 ms. We were unable to time the gate to the early ignition of the THKP. Spectra are shown below in Fig. 3-10 that represent either the plasma from the SCB or the complete late ignition characterized by its broadband emission. We are unable to make any conclusions about whether or not any electronic energy contributed to the ignition, but it is unlikely given the long function times and the short-lived emission from the plasma.

3.4 - CONCLUSIONS

These tests were performed to examine the likelihood of electronic energy transfer from the SCB plasma contributing to the ignition of EMs containing metal atoms. The data suggest that such energy transfer was observed in BNCP and ZPP. It cannot be ruled out for CP and seems unlikely for THKP. A more definitive study would need to include characterization of the emission spectra for both CP and BNCP. It would also be facilitated by an easier way to time the collection of the emission to the ignition event.

3.5 – ACKNOWLEDGEMENTS

We gratefully acknowledge the help of Dave Wackerbarth for pressing energetic materials in SCB devices for the spectroscopic study, Dr. Bernardo-Tovar, of SCB Technologies for providing and mounting SCB devices, and Mike Alessio of EBCo for providing ZPP-loaded devices. We are also grateful to John Fronabarger for helpful discussions on BNCP and CP electronic absorptions.

3.6 - REFERENCES

1. D. A. Benson, M. E. Larsen, A. M. Renlund, and R. W.Bickes, Jr., J.Appl. Phys. 62, 1622 (1987).
2. Private Communication, John Fronabarger, Pacific Scientific.
3. R. W. B. Pearse and A.G. Gaydon, "The Identification of Molecular Spectra," Chapman and Hall, Ltd., London, 1976..

(THIS PAGE INTENTIONALLY LEFT BLANK)

3.7 - FIGURES

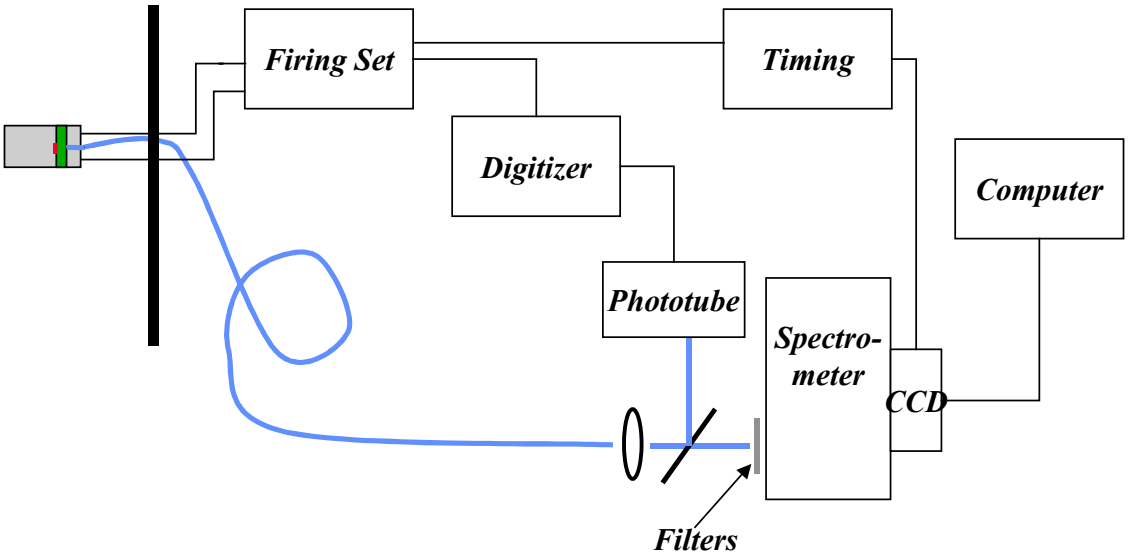

Figure 3- 1. Schematic of experimental arrangement.

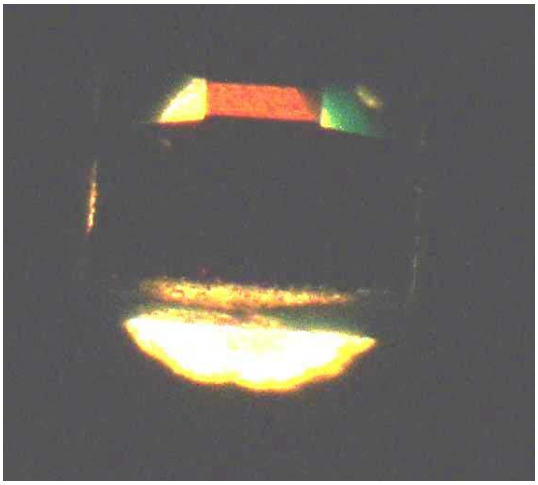

Figure 3- 2. Image through microscope of optical fiber back-lighting SCB to check for alignment.

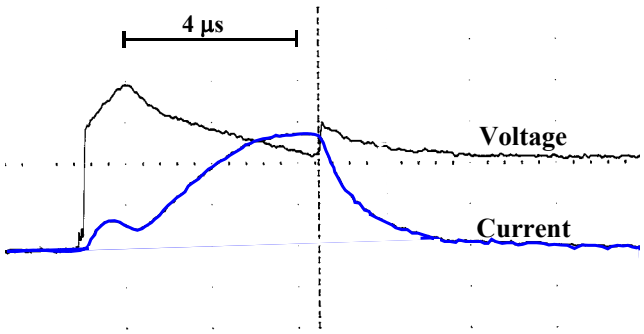

Figure 3- 3. Typical current and voltage waveforms for SCB firing. The peak voltage was 40V.

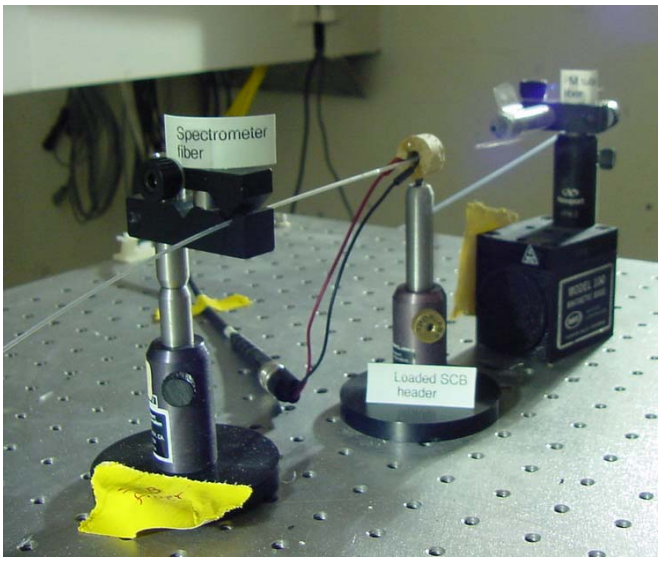

Figure 3- 4. Photograph of set-up. The loaded SCB device was mounted in a wooden fixture for ease of positioning. The electrical leads for firing the SCB are shown (the red and black ones) and the fiber carrying the spectral information was inserted between the leads. The other fiber was used to indicate the completion of the explosive event at the output face.

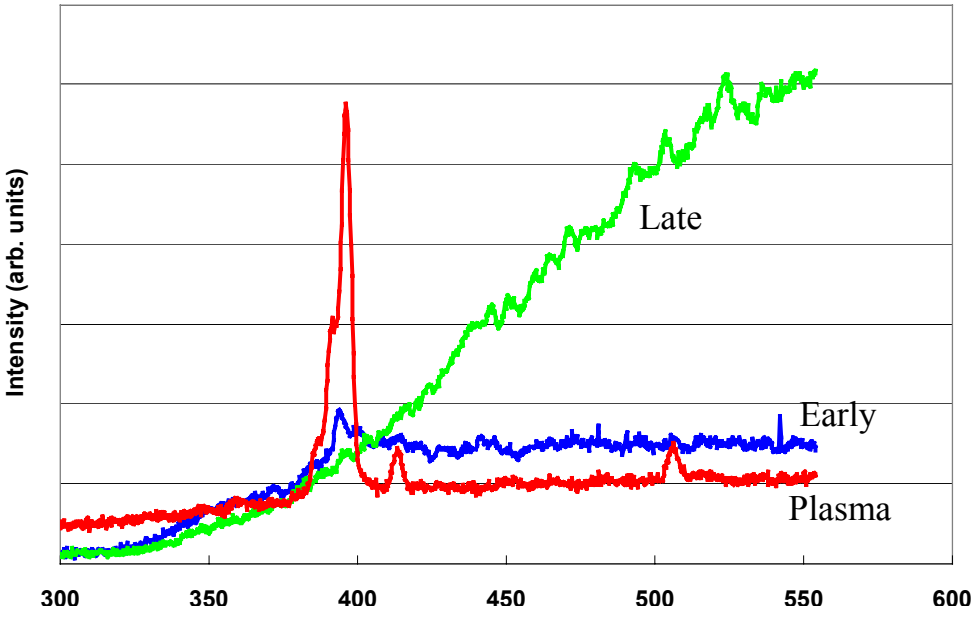

Figure 3- 5. Emission spectra, through the silicon-on-sapphire substrate, from a type 70A2A SCB firing of CP. "Early" and "Late" refer to different gate times relative to the ignition event, however, the "Plasma" spectrum precedes both of the others.

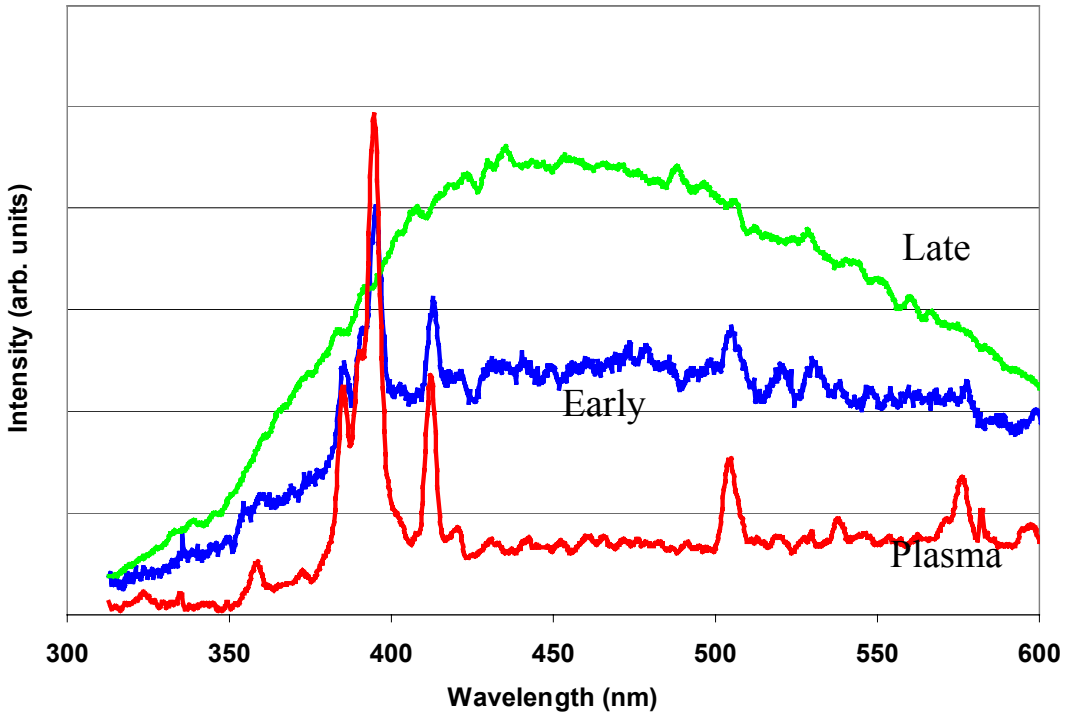

Figure 3- 6. Emission spectra from a Type 3–2B1A SCB firing of CP.

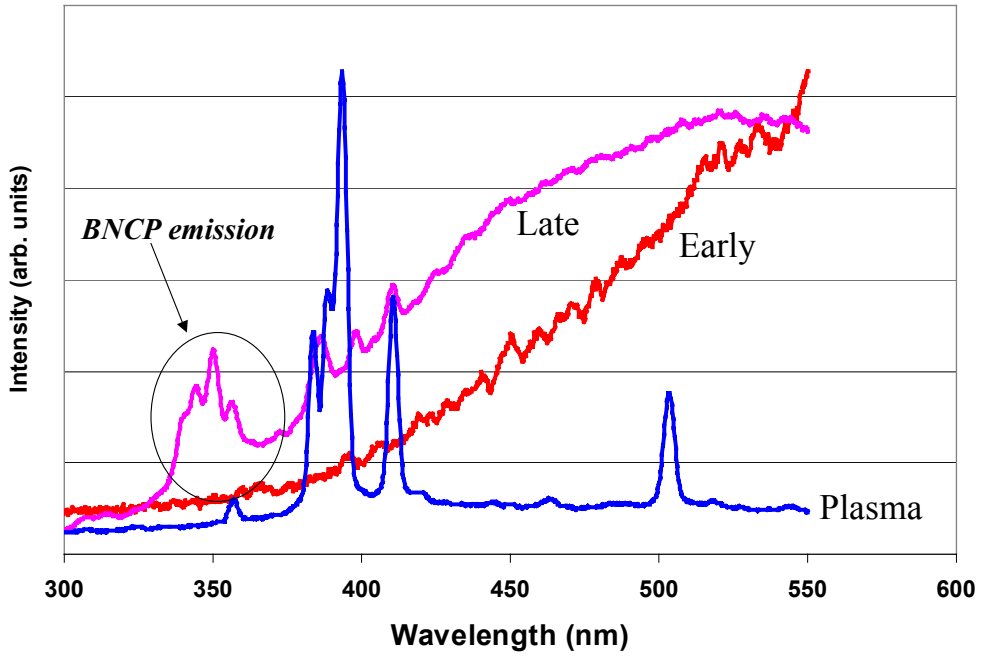

Figure 3- 7. Emission spectra from a Type 70A2A SCB firing of BNCP. In these spectra, the "Early" spectrum precedes the "Plasma" spectrum in time.

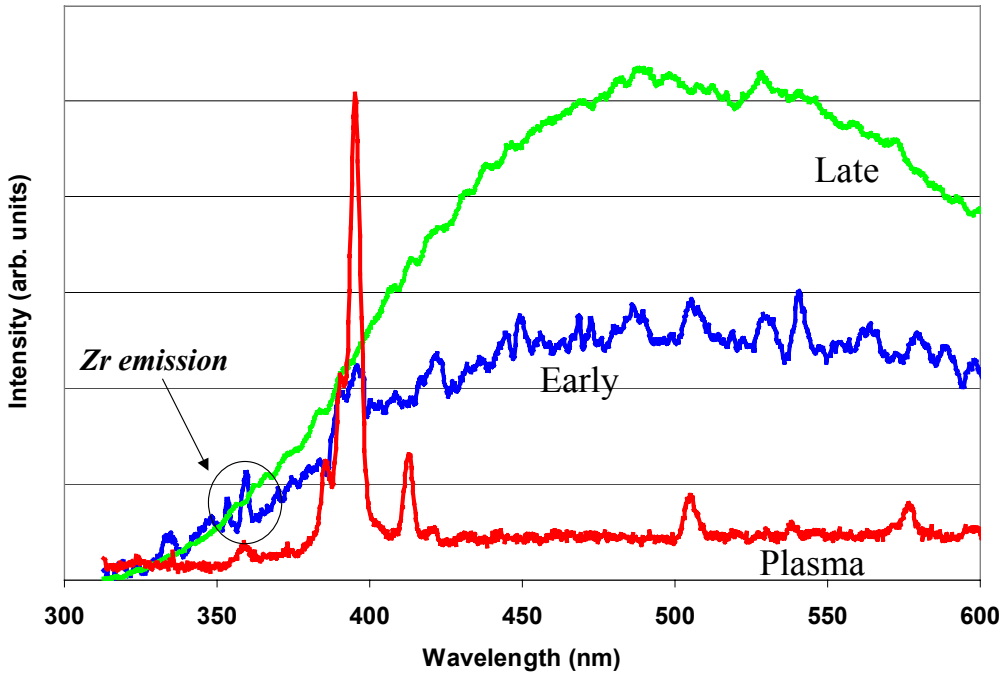

Figure 3- 8. Spectra from Type 70A2A SCB ignition of ZPP.

Figure 3- 9. Pictures of charge holders after firing, showing damage from the explosive events.

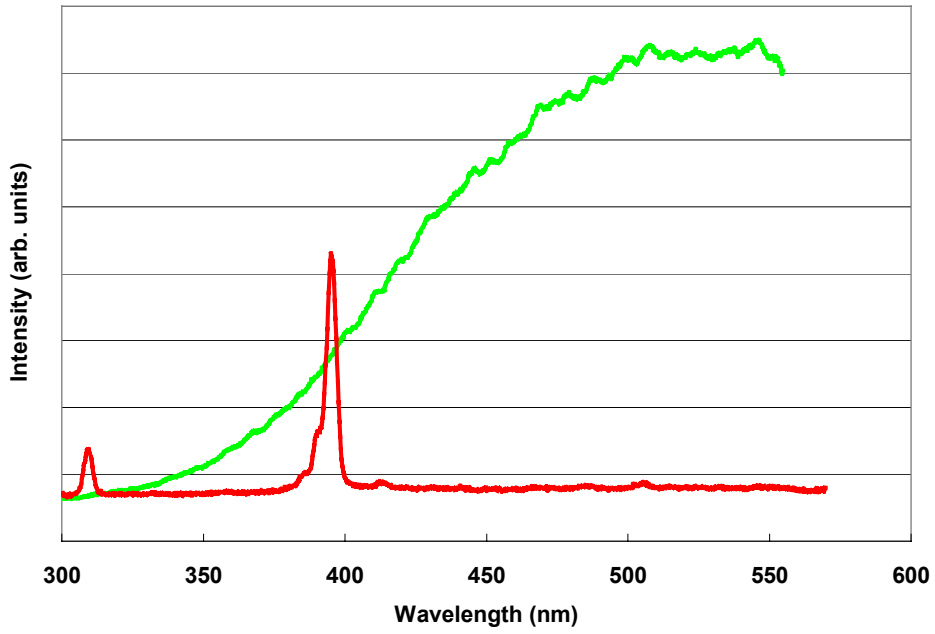

Figure 3- 10. Emission from plasma and complete ignition of THKP from a Type 70A2A SCB.

(THIS PAGE INTENTIONALLY LEFT BLANK)

4.0 – Task 3, SMART SCB COMPONENT DEVELOPMENT

Daniel J. Savignon†
Sandia National Laboratories
P.O. Box 5800
Albuquerque, NM 87185-1454

ABSTRACT

For applications requiring the ignition of energetic materials, semiconductor bridge (SCB) initiators have proven to be an attractive alternative to metal bridgewires. Compared to metal bridgewires, SCBs operate with reduced voltage and energy requirements[1]. Comprised of thick (typically 2 μm) polycrystalline silicon ("polysilicon") the SCB is fabricated with the same material deposition and etch techniques employed in microelectronics processing. This fact leads to the possibility of making a "smart SCB component" by integrating fire-control/power switching circuitry and state-of-health sensors onto the SCB die. The objective of Task 3 of CRADA SC98/01540 was to design, build and characterize a smart SCB ignition device for DOE/DP and commercial applications. This report summarizes the work accomplished.

4.1 - INTRODUCTION

The name "smart SCB component" implies an SCB device that can continuously monitor its state-of-health and, once enabled, control its own firing based on environmental inputs or a timed delay relative to some reference event. Desirable elements in a smart SCB component include: an initiation switch, an explosive powder sensor, a communications-port, memory, a timer, and a render-safe mechanism (energy shunt, for example). Figure 4-1 shows a block diagram of a generic smart SCB integrated circuit (IC) with these elements. For additional security other devices such as a mechanical latch could be placed in the power delivery path.

In order to develop a smart SCB IC, a suitable fabrication process sequence must be available. The processes must be capable of realizing both a thick polysilicon layer (for the SCB) and standard CMOS circuitry to make the smart functions mentioned above. The thickest polysilicon layers available in standard CMOS processes are about 1/7 of what is required to make traditional SCBs. On the other hand, micro-electro-mechanical

†Present Address: Analog Devices Inc., 7910 Triad Center Drive, Greensboro, NC 27409-9605

systems (MEMS) processes make mechanical polysilicon components that are similar in thickness to SCBs. Sandia has been a leader in developing a process that integrates MEMS and CMOS circuitry onto the same die. This process is referred to as an integrated MEMS or IMEMS process. A cross-sectional view of an IMEMS process is shown in Fig. 4-2. First the MEMS devices are fabricated in a deep trench and then, after high temperature annealing to remove residual stresses, the CMOS device processing is performed on the surface.

Based on outcomes from initial CRADA meetings with our commercial and DP partners it was decided to focus the initial Task 3 work on developing the initiating switch and the explosive powder sensor. The communications port, digital control logic and volatile memory were left to be defined later in the CRADA schedule when a specific application was to be chosen. This made sense since these latter blocks are relatively straightforward to implement with standard CMOS circuitry.

From the onset of the CRADA Sandia decided that it would do Task 3 development work that fell within the constraints of existing Sandia Microelectronics Development Laboratory (MDL) processes which, at the beginning of the CRADA, included the existing IMEMS and CMOS6R processes. In other words, no major process enhancements/modifications would be made to the existing MDL processes since the CRADA funding and schedule did not allow for this. However, Sandia did make the most of the CRADA Task 3 funding by prototyping initiating switch test devices on "extra" space on other project's outgoing reticle sets. This provided considerable leverage for the CRADA Task 3 funding since no processing costs were incurred for the fabrication of the initiation switch test devices.

Midway through the CRADA, Sandia's MDL experienced a shift in funding priorities (unrelated to the funding of this CRADA) that cancelled all work on existing and future IMEMS processes. This meant that the original smart SCB concept (as depicted in Fig. 4-1) could not be developed since there was no process in which to fabricate it. During a subsequent meeting with our CRADA partner (The Ensign–Bickford Co.), the Sandia Task 3 staff proposed a smart SCB design that would not require an IMEMS process. The proposed design would have an SCB, an explosive powder sensor and a cracked-die sensor, all of which could be processed on a single die in the MDL's SUMMiT- IV (MEMS only) process. Although the modified design would not feature CMOS circuit blocks the powder sensor and cracked-die sensor would provide two different state-of-health detection mechanisms that could be interrogated by off-chip circuitry both in a production or deployed environment.

The CRADA Task 3 work was grouped into three efforts. The first effort consisted of designing, fabricating and evaluating several large initiation switches at the MDL. The second effort sought to investigate the resilience of existing IMEMS dice to high explosive powder pressing pressures. And finally, using a Sandia MEMS-only process, smart SCB components were designed, fabricated and evaluated.

4.2 - INITIATION SWITCH DESIGN AND EVALUATION

Passing a large current (one to ten amperes) for tens of microseconds through an SCB produces a hot plasma capable of igniting explosives**.** To handle currents of one ampere or larger, the SCB initiation switch is typically a power device such as a silicon controlled rectifier (SCR) or power MOSFET.

It is not uncommon for SCB initiation voltages and currents to be greater than 20 Volts and 10 Amperes, respectively.[3] These are very high values when compared to the ratings of traditional CMOS integrated circuit technologies with feature sizes below 1.0 µm. A typical drain-to-source *voltage rating* ($V_{ds\text{-}max}$) of a 0.6µm CMOS transistor is 5 Volts. This means a MOSFET device made in such a process can only "block" or hold-off 5 Volts when the device is turned off. This limitation is fixed by the fabrication process and cannot be altered by the designer. On the other hand, the *current rating* of a MOSFET can be increased by the designer by making the device channel width-to-length ratio (W/L) very large. In summary, the CMOS process sets the device voltage rating but the designer is free to size the device to handle a particular current rating.

Two different initiation switches were designed in Sandia MDL processes and fabricated on "extra" space on other project reticles. The first design was fabricated in the IMEMS process since this was the originally-targeted technology in which to develop a smart SCB component. Fig. 4-3 shows the layout of reticle set RS205 and the location and features of the large n-channel MOSFET device that was fabricated. This transistor had 125 gate fingers each with a length of 2 µm and a width of 257 µm giving the whole device an equivalent W/L ratio of (32,125/2) or 16,062. For the MDL's IMEMS process, a standard MOSFET device with a W/L ratio of 16.7 will pass 6 mA of current with a drain-source voltage of 5 Volts (this means the standard device's on-resistance is about 5 volts/6 mA or 830 ohms. With a W/L ratio of 16,062 this large MOSFET should, in theory, pass [(16,062/16.7) * 6mA] or 5.8 Amps yielding an on-resistance of about 5 volts/5.8Amps or 0.86 ohms. However, measurements made on the RS205 large MOSFET using an HP4145 parameter analyzer showed an on-resistance of about 2 ohms. From this data it can be concluded that the device W/L ratio scaling is not linear when devices this large are being developed, possibly because of parasitic effects of contact resistance and resistances of buried layers. The net result is that the device would need to be re-sized to yield a significant decrease in on-resistance. To ensure that the majority of the energy is dissipated in the SCB during firing, a desirable initiation switch on-resistance is 0.1 ohm or lower since the SCBs typically have resistances of about 1 ohm. This means that the MOSFET would have to be about 20 times larger than the one fabricated in the IMEMS RS205 experiment.

A second initiation switch design was fabricated in the Sandia MDL CMOS6R process since the Sandia MDL intended to develop IMEMS capability in this technology. Fig. 4-4 shows a large p-channel MOSFET device that was fabricated on reticle set RS206. This device was designed with 8 blocks, each containing 778 unit transistors. The unit transistors had gate lengths of 1.2µm and gate widths of 100µm. The total W/L ratio was therefore (8*778*100µm)/(1.2µm) or 518,667. A standard (20µm/1.2µm) p-MOSFET

CMOS6R device will pass a maximum of 2mA of current with 5 Volts across its source and drain, making its on-resistance 5V/2mA or 2500 ohms. Since the large device is 31,120 times larger from a current drive standpoint its predicted on-resistance would be (2500 ohms)/31,120 or approximately 0.1 ohms. Measurements of this second large initiation switch yielded on-resistance values of 0.7 ohm. Again, the measured on-resistance value fell short of what was predicted, probably because of parasitic effects. In order to get to an on-resistance of 0.1 ohm the CMOS6R device would need to be about 7 times larger. .

Commercial integrated circuit processes that specialize in power MOSFET devices use novel designs and put device contacts on both sides of the wafer (source and gate contacts on top and drain contacts on the bottom) giving rise to what is known as a vertical MOSFET[4]. The commercial devices are much more area efficient when compared to what is possible using standard signal-processing CMOS, like those in the Sandia MDL.

To get MOSFET on-resistances of 0.1 ohm and lower with the CMOS6R process, the devices would need to be much larger than the 2 mm by 3.5 mm device shown in Fig. 4-4 For any smart SCB component designed on a single die within Sandia's traditional CMOS process, the initiation switch would consume a very large area and would render a total die area that is 10 – 15 times as big as an SCB-alone die[1]. The prospect of such large smart SCB component dice raises questions as to the viability of packing such large surface areas with explosive powder at the typical powder pressing pressure of 20 kpsi. Instead, it would be wise to develop power MOSFETs with alternative designs.

4.3 - IMEMS RS111 DICE PRESSING TESTS

The goal of these tests was to determine if large IMEMS dice would survive explosive powder pressing loads. IMEMS accelerometer dice from reticle set RS111 (fabricated several years earlier for another unrelated project) were used to represent a smart SCB component with thick poly devices and CMOS circuitry. These IMEMS dice were mounted on large, 0.445" diameter by 0.500" deep, headers at SCB Technologies. The units were loaded with CP explosive powder at pressures of 1kpsi, 5kpsi, and 10kpsi. Nominal pressing pressures are in the range of 20kpsi to 40kpsi. With the initial pressings complete, the powder was washed out with isopropyl alcohol. The devices were inspected and photographed for visual damage. The press used was a UA2234 pressure control system and a 339312 Powder Compaction Test Fixture located in the Explosive Components Facility .

There were some uncertainties about the survivability of the devices at the nominal pressing pressures of 20kpsi to 40kpsi. Low pressing pressures of 1kpsi, 5kpsi, and 10kpsi were used as a starting point to determine if the devices could survive. Fig. 4-5 shows the reticle RS111 layout and one of the dice that was pressed to 5 kpsi. A crack across the top half of the die (through the microelectronics) is evident in this photo. Shown in Fig. 4-6 is a die that was pressed to 10 kpsi. Severe cracking

throughout this die is evident and the close-up of the accelerometer plate shows the localized cracking and chipping.

There are several possibilities as to why these dice are cracking at pressing pressures well below the nominal 20-40 kpsi range. First, the MEMS accelerometer plates on these particular die were designed for an entirely different application with stress limits well below the 5 kpsi and 10 kpsi that they were subjected to in this test. Secondly, die mounting issues such as epoxy voids and header surface smoothness might be more critical since the dice under test were relatively large compared to traditional SCB-only dice. In addition, the MEMS trench on these IMEMS process dice (see Fig. 4-2) presents a sharp angle deep in the dice that perhaps acts as a stress concentrator during the explosive powder pressing. The damage observed in these packed dice suggests that die mounting, die topography, and die area need to be further investigated as to how they affect smart SCB die survivability of powder pressing.

4.4 - SUMMiT-IV SMART SCB COMPONENT DESIGN

As mentioned in the introduction, the shift in funding priorities experienced by Sandia's MDL led to the cancellation of all work on existing and future IMEMS processes. Since there was now no process in which to fabricate the original smart SCB concept (as depicted in Fig. 4-1), Sandia Task 3 staff proposed a different smart SCB component design that did not require an IMEMS process. This proposed design would have an SCB device, an explosive powder sensor and a cracked-die sensor, all of which could be processed on a single die in the MDL's SUMMiT- IV (MEMS only) process. Although this amended design would not feature CMOS circuit blocks, the powder sensor and cracked-die sensor would provide two different state-of-health detection mechanisms that could be interrogated by off-chip circuitry both in a production or deployed environment.

Sandia's SUMMiT – IV process is a four-level polysilicon MEMS process. Figure 4-7 shows the layers of polysilicon and sacrificial oxides for this process.

Figure 4-8 shows the entire module that was fabricated on reticle set RS225 (consisting of 12 individual dice that were identical except for the powder sensor designs) and a close-up of an individual die with the SCB, powder sensor, and cracked-chip sensor.

The cracked-chip sensor consists of a 50 um wide poly0 strip that encircles the entire smart SCB die. Electric continuity is monitored between pads C and D (see Fig. 4-8). Approximately 2 kohm of resistance will be measured across these pads (around the cracked-chip loop) so long as no die cracking/breakage (loop breakage) occurs.

The SCB is accessed from pads A and B. Putting a voltage source across or a current source through these pads causes SCB initiation.

Powder sensor continuity is checked across pads C and B. The C pad is connected to a flexible beam that is suspended 2um above a strip of poly0. The poly0 strip is connected to pad B. When explosive powder is pressed onto the smart SCB system die the flexible

beam bends and its midpoint moves the 2um distance to contact the poly0 strip. The beam is supported on each side by a support pad with very rigid features.[6] To a first order approximation the beam and support pads are treated as a "fixed-fixed supported beam." This approximation was used to roughly estimate how much different beam lengths would deflect for a given powder packing load level.[7]

Figure 4-9 shows top and cross-sectional views of the two different powder sensor designs. The Type-A powder sensor beam is 53 um wide and consists of an I-beam cross –sectional stack of poly1/poly2 and poly3. Because of its width the type-A beam has etch-release holes that ensure the sacrificial oxide 1 (SACOX1) and sacrificial oxide 3 (SACOX3) are completely etched away. The Type-B powder sensor beam is also an I-beam cross-sectional stack of poly1/poly2 and poly3 but is narrower than the type-A beam by 24um and does not have etch-release holes (see Fig. 4-9). The lack of etch-release holes on the poly3 layer leaves a trapped oxide between the poly1/poly2 and poly3 layers as shown in Fig. 4-9. The type-B beam is narrow enough that even without etch-release holes in the lower poly1/poly2 layer the SACOX1 layer will be completely etched away. Both the type-A and B powder sensor beams are supported by the same design of rigid pads. These pads are made rigid by the fact they are composed of stacked layers of poly0, poly1, poly2, and poly3 with minimum width oxide cuts and have trapped oxide within the poly stack (see Fig. 4-9). Both the type-A and type-B powder sensor beam designs were made in 6 different lengths: 75um, 100um, 125um, 150um, 175um, and 200um.

Figure 4-9 also shows that each powder sensor has a fence running parallel to each side of the beam. Made with simple stacks comprised of all 4 poly layers, these fences are intended to keep powder from squeezing underneath the powder sensor beam during the powder loading process and preventing the electrical contact between the beam and the poly0 strip.

Figure 4-10 shows photographs of the fabricated type-A and type-B powder sensors next to each other for comparison. The powder fences running parallel to the powder sensor beams are visible.

4.5 - SUMMiT-IV SMART SCB COMPONENT PRESSING TESTS

4.5 - 1 - MODULE PRESSING TESTS

In order to evaluate the SUMMiT-IV smart SCB system designs, two different powder pressing test approaches were used. The first approach was to mount and powder press the entire SUMMiT-IV module (one piece of silicon with all twelve (12) smart SCB systems present (as shown in Fig. 4-8). The second approach was to saw the modules into the individual smart SCB components and press the individual dice while monitoring the powder and cracked-die sensor resistances. This second approach is described in section 4.5-2.

Three of the SUMMiT-IV modules were mounted on large, 0.445" diameter by 0.500" deep, headers at SCB Technologies. The press used was a UA2234 pressure control system and a 339312 Powder Compaction Test Fixture located at Sandia in the Explosive Components Facility. Powdered sugar was used as a packing powder to simplify safety and clean-up procedures. Two of the three units were packed to 5kpsi and the third module was packed to 10 kpsi. After rinsing the modules with hot water (to wash away the powdered sugar) the individual smart SCB systems were visually inspected.

From a macro-view the modules looked very good with no cracking. However, close-up views at the various powder sensors revealed a definite pattern. For all three modules, every type-A powder sensor beam (regardless of length) was either slightly or severely cracked and damaged, whereas visual inspections of all the type-B powder sensor beams revealed no damage whatsoever. Figure 4-11 shows photographs of a smart SCB component with a type-A powder sensor. No damage to the cracked-chip sensor, the SCB or the bond pads is evident. On the other hand, the powder sensor beam is clearly damaged. This particular device had been packed to 5 kpsi. The remaining type-A powder sensor beams also showed similar damage. Figure 4-12 shows photographs of the 200um long (longest and therefore most flexible) type-A and type-B powder sensors from the third module that was packed to 10 kpsi. The type-A beam is clearly damaged whereas, the type-B beam is intact. It should be noted that the photograph of the type-B sensor does show some surrounding damage such as the missing powder fence (above the beam) and some chipping from the perimeter of the right side powder sensor support pad.

4.5 -2 - WIRE-BONDED-DICE PRESSING TESTS

The results from pressing the three modules with all the smart SCB designs clearly showed that the Type-A powder sensors did not hold up to the relatively low pressing pressures of 5 and 10 kpsi, whereas the type-B powder sensors showed no damage at all. To further investigate the type-B powder sensor response, individual smart SCB component dice were mounted on headers and wire bonded such that their cracked-chip and powder sensor resistances could be monitored during powder pressing. It must be noted that the SUMMiT-IV MEMS process does not include a metal layer so the bond pads had no metal layer to facilitate wire bonding. Sandia does have capabilities to post-metalize a MEMS process but the alignment accuracy is not sufficient to properly define the SCB poly dimensions. This is why the SCBs themselves were not evaluated. Despite these issues, 5-mil bond wires were successfully bonded straight to the poly3 layer. Figure 4-13 shows a photograph of one individual smart SCB component die mounted on a header and wire bonded. The individual dice that were selected for this test included the following designs: A75, B75, B100, B150, and B200 (the letter represents the powder sensor beam design, type-A versus type-B, and the number is the length, in micrometers, of the powder sensor beam).

It is important to note that these individual dice were obtained by sawing the Sandia SUMMiT-IV MEMS modules *after* the MEMS release process (etching away of the sacrificial oxide layers to free the powder sensor beams). Sandia's SUMMiT-IV MEMS

process is set up to only provide 4.6mm x 4.6mm modules (as shown is Fig. 4-8) as a final product. Sawing after the release process is very risky since typical MEMS devices such as gears and levers are likely to be damaged. Both of the B125 dice did not pass visual inspections after being sawed so they were not chosen to be mounted and wire-bonded. Both of the B175 dice had powder sensors that indicated a short circuit prior to being packed so, most likely, foreign material from the sawing process lodged between the beam and the bottom plate. For these reasons the B125 and B175 units were absent from this second set of pressing tests.

Shown in Fig. 4-14 is pre- and post-pressing photographs of the A75 die. Before being pressed the powder sensor beam is clearly undamaged. During pressing the cracked-die and powder sensor resistances were monitored. The cracked-die sensor resistance measured 2.2 kohm before powder pressing and never changed throughout the pressing process. This indicated that the A75 die did not crack in a way that would open circuit the sensor loop. A visual inspection of the die after pressing showed no die cracking whatsoever. The A75 die powder sensor resistance was infinite (open circuit) prior to powder pressing and at a powder pressure of 4.5 kpsi the powder sensor resistance went from infinite to 100 kohm of resistance. The pressing pressure was increased for the A75 device until the powder sensor resistance reached a value of 250 ohm at which time increasing the pressing pressure did not cause any further decrease in the powder sensor resistance. The pressing pressure at this final point was 8 kpsi. The post-pressing photograph in Fig. 4-14 shows cracking in both the top and bottom halves of the powder sensor beam. The cracks appear to originate from etch-release holes in the top surface.

Evaluations of the B75, B100, B150, and B200 devices were carried out in a similar fashion. The resistance of each die's powder sensor and cracked-die sensor was monitored while the pressing pressure was slowly increased. For every B-type die the cracked-die sensor resistance measured 2.2 kohm before pressing and remained constant all the way to the final maximum pressing pressure. Post-pressing visual inspections of each die confirmed that, indeed, no die cracking had occurred. Plots of the B-type powder sensor resistances versus pressing pressures (loading) is shown in Fig. 4-15. As expected, longer powder sensor beams reach their minimum resistance at lower powder pressing pressures than do shorter beams. The B200 sensor reached minimum resistance at 2.5 kpsi of loading, while the B100 and B150 sensors reached minimum resistances at about 8 kpsi of loading. Since the B75 powder sensor reached minimum resistance at 14 kpsi its response would be the closest to what is needed in practical applications where most powders are pressed to 20 kpsi and higher.

Shown in Figs. 16 through 19 are pre- and post-pressing photographs of the B75, B100, B150, and B200 powder sensor beams. In every case the powder sensor beam and powder fences appear undamaged in the post-pressing photograph. With the exception of the B200 die each of the type-B powder sensor resistances measured as an "open-circuit" when checked *after* washing the powder from the die. After being rinsed the B200 powder sensor resistance measured 12 kohm. This, most likely, is due to powdered sugar/water residue wedged between the powder sensor beam and the poly0 strip underneath.

4.6 - TRANSFERRING SMART SCB PROCESSING TO INDUSTRY

For any commercial entity that wants to continue the type of work described in this report there are several routes by which this is possible. One route is to purchase module space (for prototyping use only) on the Sandia SUMMiT-IV or SUMMiT-V MEMS processes. Designs are captured and communicated to Sandia using AutoCAD® ".dwg" files. Throughout the year Sandia offers basic and advanced classes on designing within the SUMMiT MEMS processes.

Another option is to prototype devices with any of the growing number of commercial MEMS companies. As an example, Cronos Integrated Microsystems, Inc (www.memsrus.com) offers a 12 week turnaround time-MEMS prototyping service for a 3-layer polysilicon – surface micromachining process.[8] Designs are captured with a 2-D layout editor from Microcosm Technologies Inc. (www.memcad.com). Another company, IntelliSense Corporation (www.intellisense.com), is a developer of MEMS CAD and analysis software and provides volume manufacturing of custom MEMS devices. There are certainly more companies with similar services.

4.7 - SUMMARY AND CONCLUSIONS

The objective of Task 3 of CRADA SC98/01540 was to design, build and characterize a smart SCB ignition device for DOE/DP and commercial applications. A smart SCB component integrates fire-control and power switching circuitry directly onto an SCB die. In addition, a smart SCB component integrates sensors to enhance state-of-health monitoring of SCB detonators while in the field. Functions such as fire-control, power switching, data communication, timing, and memory storage require CMOS circuitry while the SCB requires a thick polysilicon layer. In standard CMOS processes these requirements cannot be simultaneously met. An IMEMS process on the other hand meets both of these requirements.

In regards to SCB power initiation switches, it was demonstrated that very low on-resistance traditional CMOS devices are realizable but that they require considerable die area. Initiation switch voltage ratings are constrained by the particular CMOS process in which the switches are built whereas the switch current carrying capability is dependent on device sizing. When designing low on-resistance CMOS initiation switches it is critical to use efficient layout techniques to achieve very large W/L ratios. In addition, significant source and drain metal areas are required to handle the large current densities.

Large IMEMS dice were subjected to powder pressing pressures below that typical of SCB applications. The damage observed in these packed dice suggests that die mounting,

die topography, and die area need to be further investigated as to how they affect smart SCB die survivability of powder pressing.

Due to the cancellation of all IMEMS processes, a smart SCB component with an SCB device, an explosive powder sensor and a cracked-die sensor was designed and fabricated using the MDL's SUMMiT- IV (MEMS only) process. The powder and cracked-die sensors provide two different state-of-health detection mechanisms that can be interrogated by off-chip circuitry. Powder pressing tests show that the type-A powder sensors are not a robust design but that the type-B powder sensors can survive the 20 kpsi packing environment and provide a resistance that is inversely proportional to pressing pressure.

The continued growth of the MEMS industry will provide many opportunities to further development of smart SCB systems in the commercial world. Companies exist that offer MEMS design and analysis software along with prototyping and volume manufacturing.

4.8 - ACKNOWLEDGEMENTS

Many thanks go to Stuart Smith and David Wackerbarth for arranging and performing powder packing tests at the Sandia Explosive Components Facility, Jim Allen for his assistance in mechanical design/analysis, the staff at the Sandia Microelectronics Development Laboratory for facilitating and releasing the MEMS samples in this work, Bernardo Martinez-Tovar at SCB Technologies Inc. for mounting and wire bonding the samples, Theresa Gutierrez for measuring the large MOSFET on-resistances and Wilson Barnard and Bob Bickes for their encouragement and support of Task 3 activities. Sandia is a multi-program laboratory operated by Sandia Corporation, a Lockheed Martin Company, for the United State Department of Energy under Contract DE-AC04-94AL85000.

4.9 - REFERENCES

[1]D. A. Benson, M. E. Larsen, A. M. Renlund, W. M. Trott, and R. W. Bickes, Jr. "Semiconductor Bridge: A plasma generator for the ignition of explosives," *Journ. Appl. Phys.* 62 (5), pp.1662 (1987)

[2]R.S. Bennet, Sandia MEMS Presentation, October 28,1998.

[3]K. D. Marx, R. W. Bickes, and D. E. Wackerbarth, "Characterization and Electrical Modeling of Semiconductor Bridges", Sandia National Laboratories Report SAND97-8246 (1997).

[4]J.G Kassakian, M.F. Schlecht, and G. C. Verghese, *Principles of Power Electronics,* Reading: Addison-Wesley,1991.

[5]Sandia MEMS Short Course Notes, April 13 – 15, 1999.

[6]B. D. Jensen, F. Bitsie, M. P. de Boer, "Interferometric measurement for improved understanding of boundary effects in micromachined beams," *Micromachining and Microfabrication, SPIE Vol. 3875*, Santa Clara, CA. Sept 20-22, 1999.

[7]W.C. Young, and R. J. Roark. *Roark's Formulas for Stress and Strain*. 6th ed. McGraw-Hill, New York, 1989.

[8]EDN Magazine, Page 22, March 16,2000

(THIS PAGE INTENTIONALLY LEFT BLANK)

4.10 - FIGURES

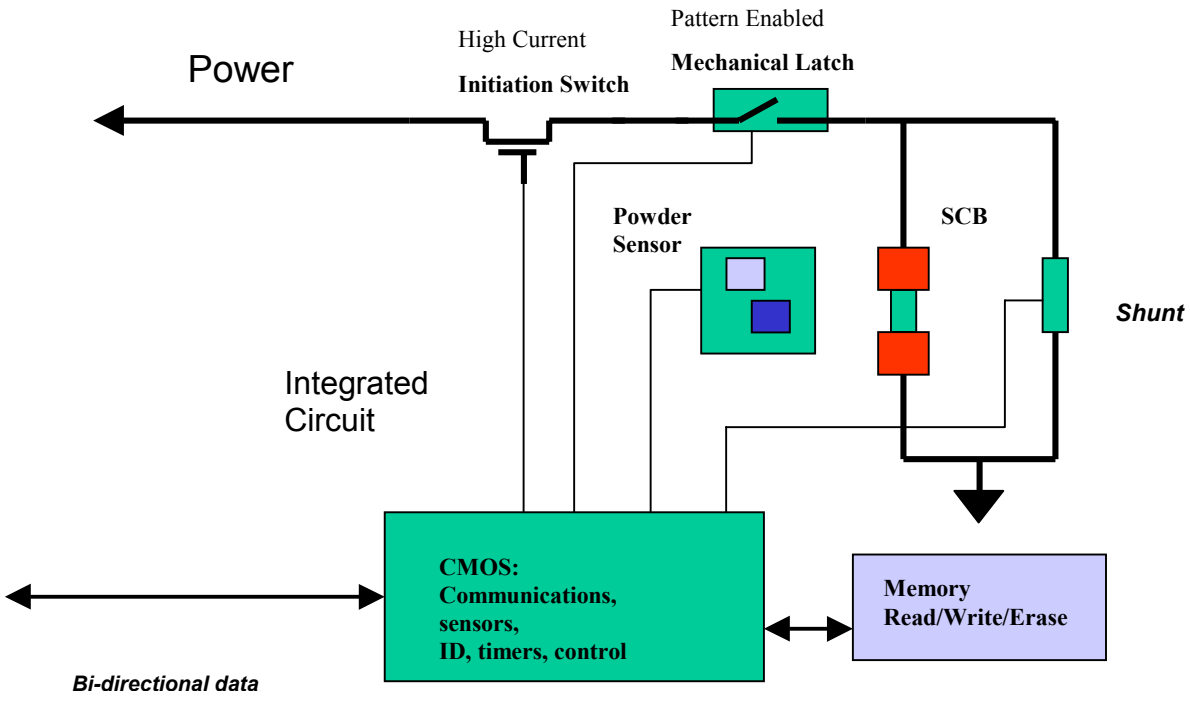

Figure 4- 1 Generic Smart SCB Integrated Circuit.

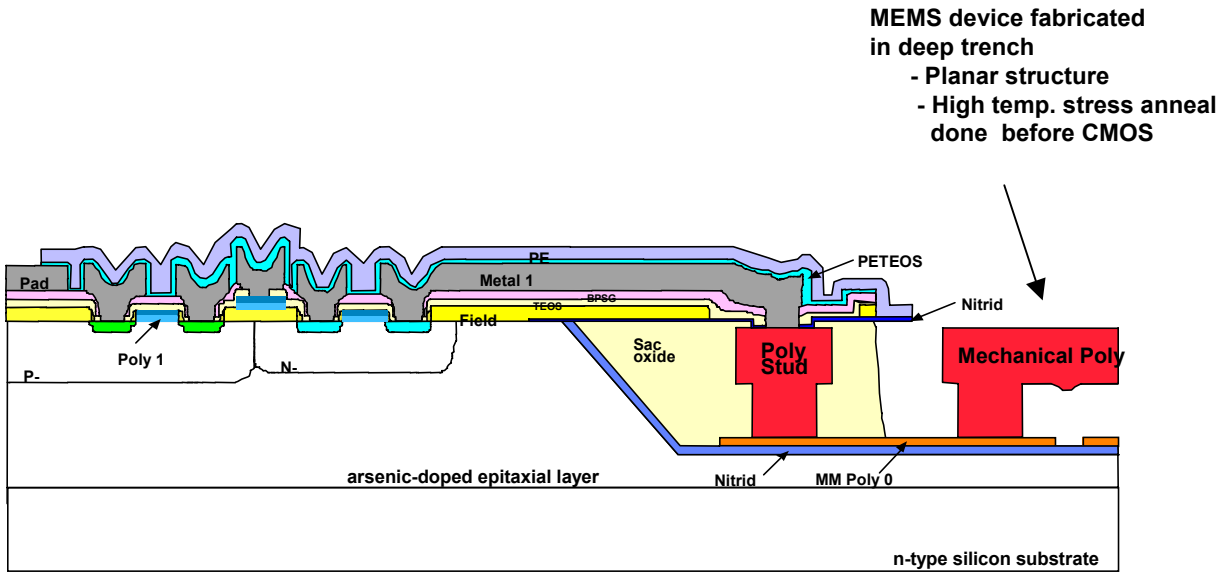

Figure 4- 2 Cross-section of IMEMS process. 2

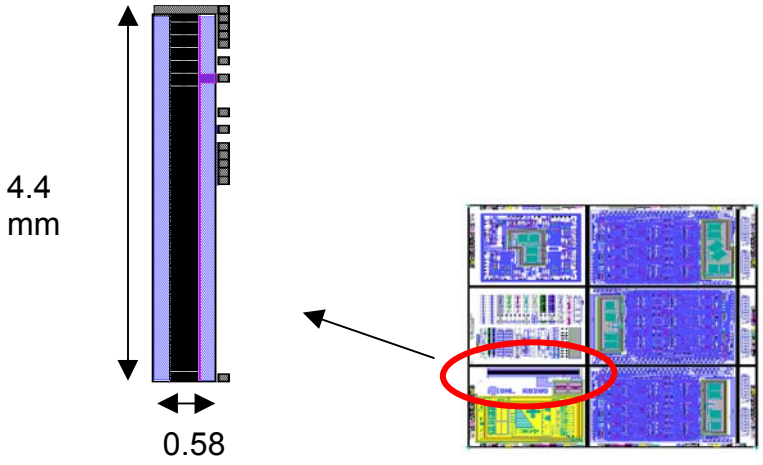

Figure 4- 3 Large NMOS on reticle set RS-205, Ron ~ 2 ohm

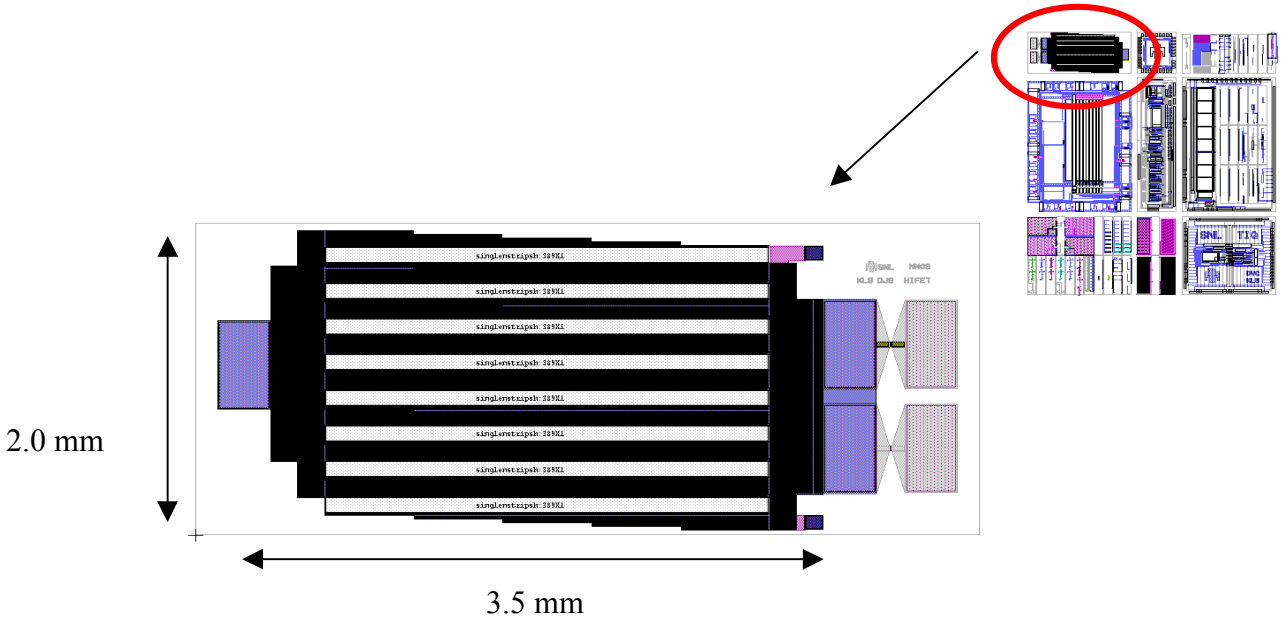

Figure 4- 4 Large PMOS on reticle set RS – 206, Ron ″0.7 ohm

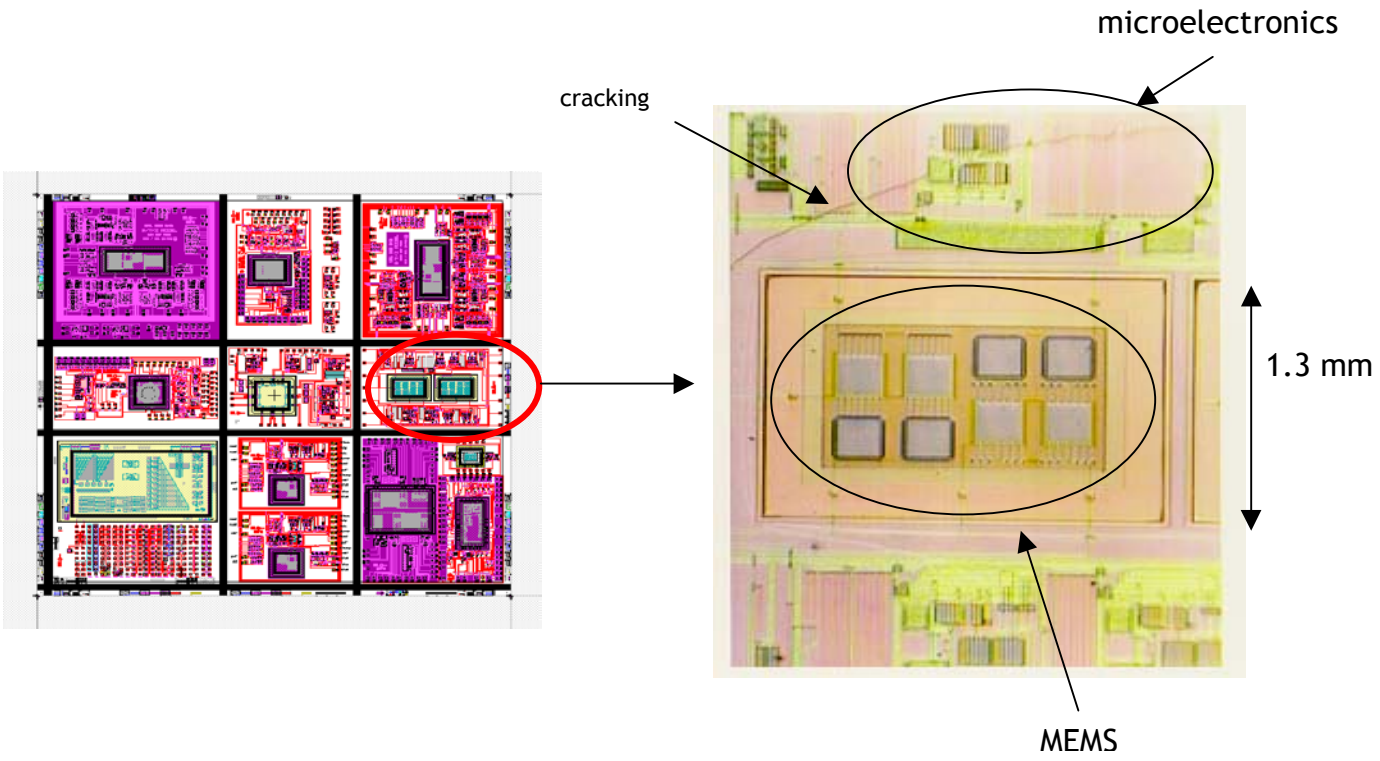

Figure 4- 5 RS -111 IMEMS reticle and chip pressed to 5 kpsi.

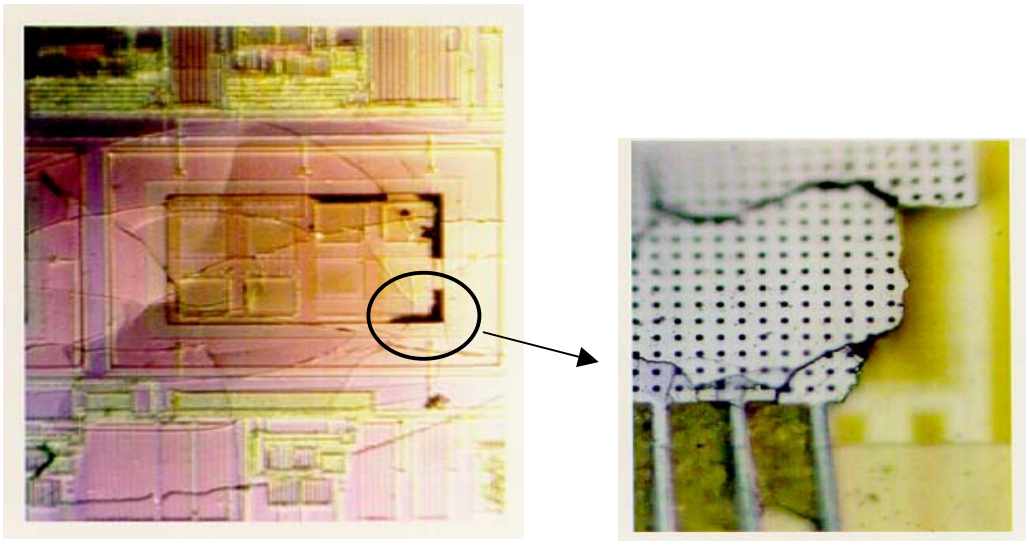

Figure 4- 6 RS-111 IMEMS chip pressed to 10 kpsi.

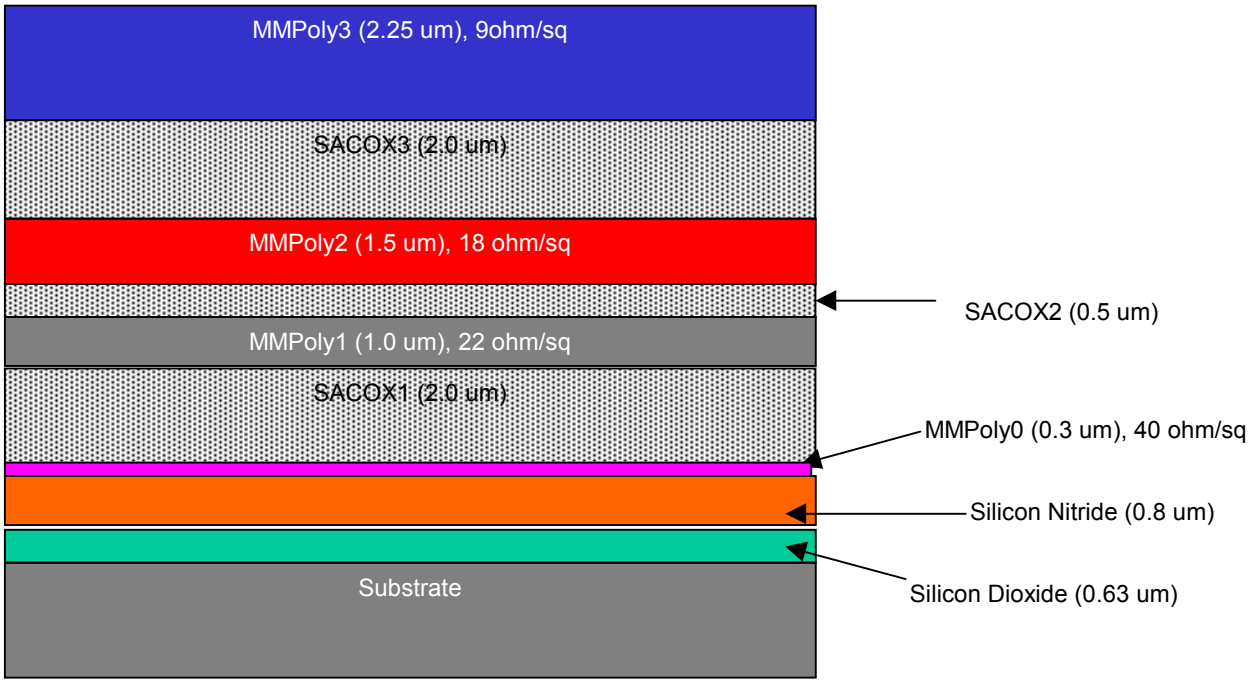

Figure 4- 7 SUMMiT -IV MEMS process layers. 5

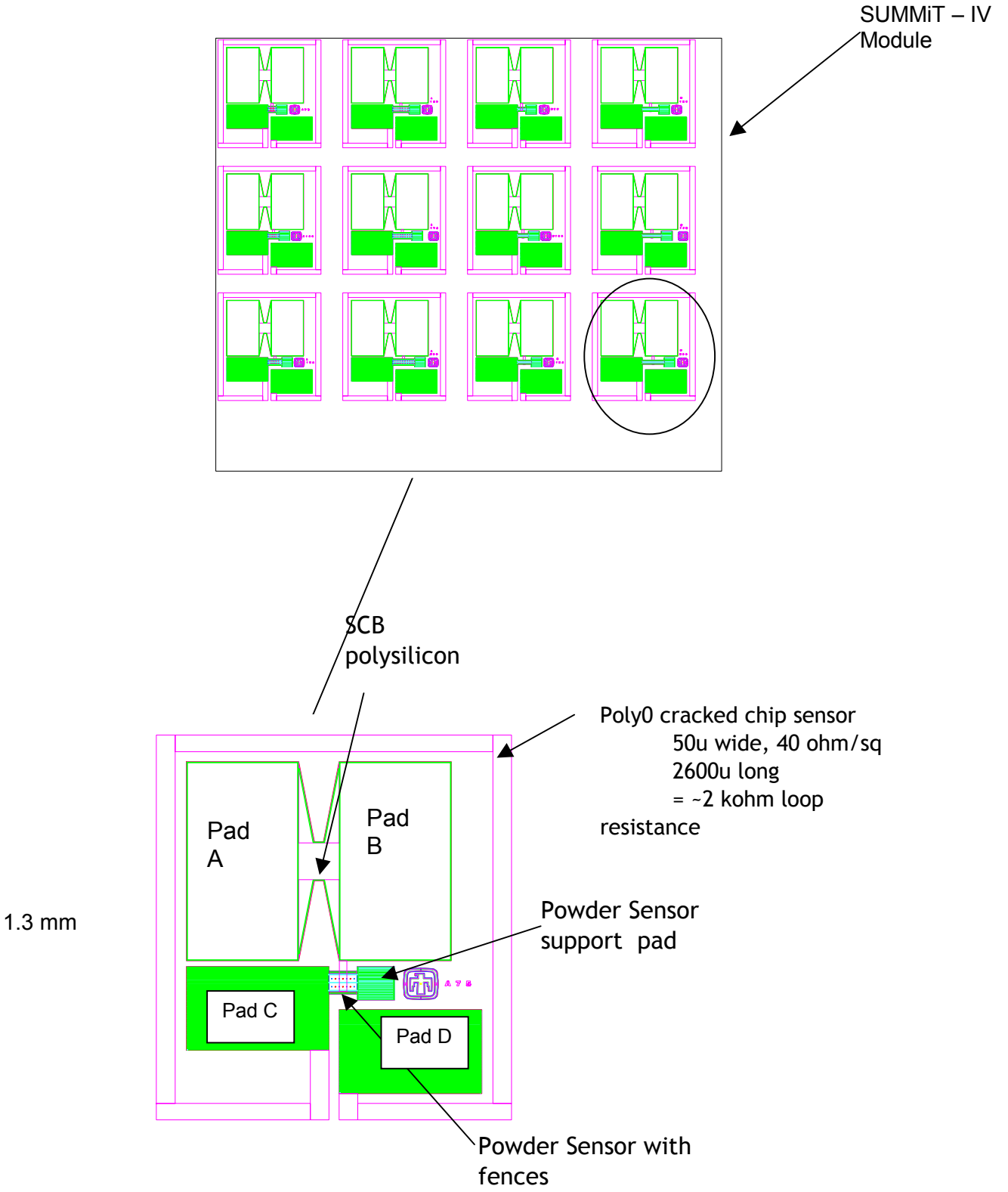

Figure 4- 8 RS-225 SUMMiT-IV module and individual smart SCB die.

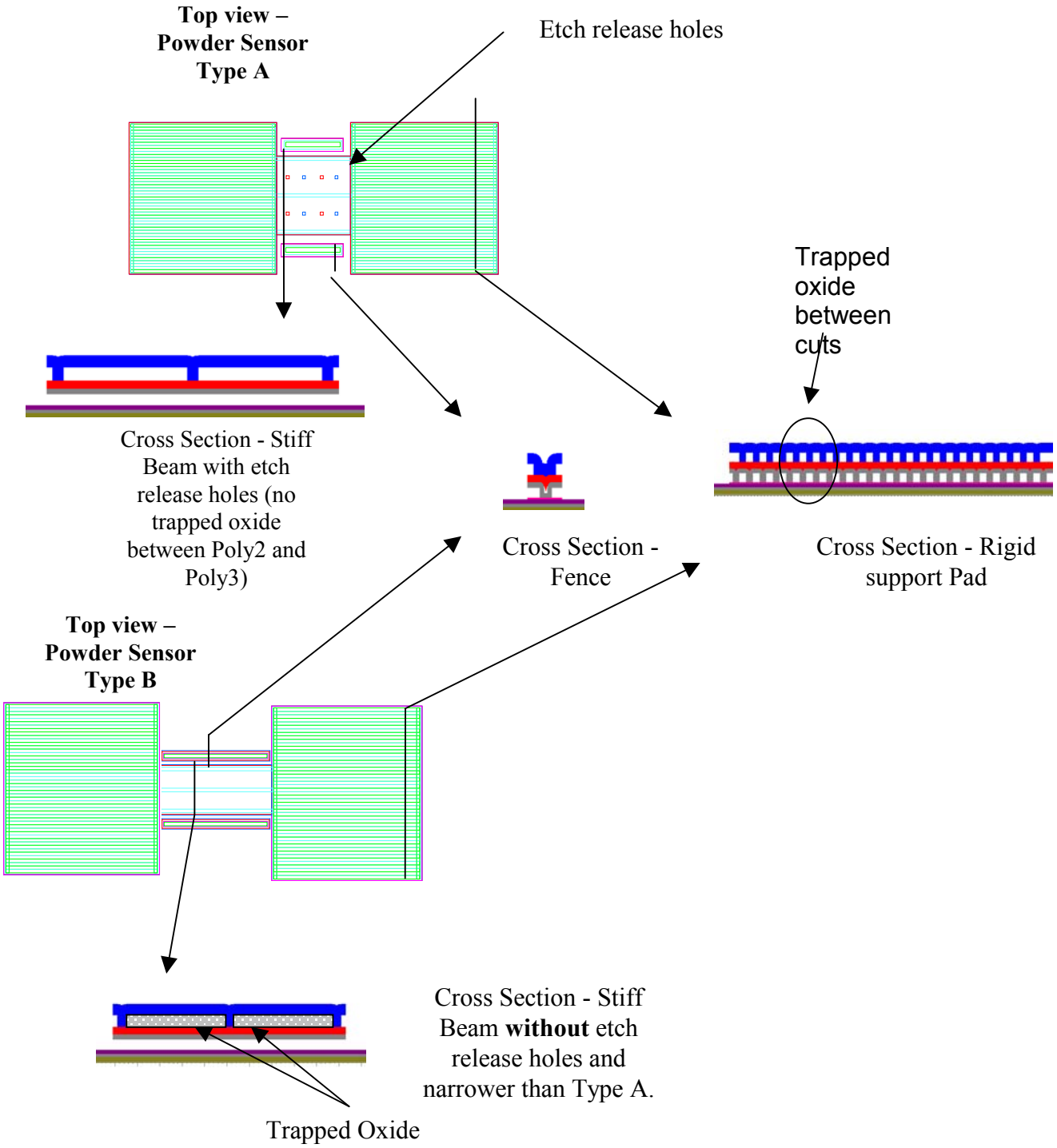

Figure 4- 9 Top and cross-section views of smart SCB Type-A and Type-B powder sensors, fences, and rigid support pads. The blue, red and brown colors indicated different poly levels.

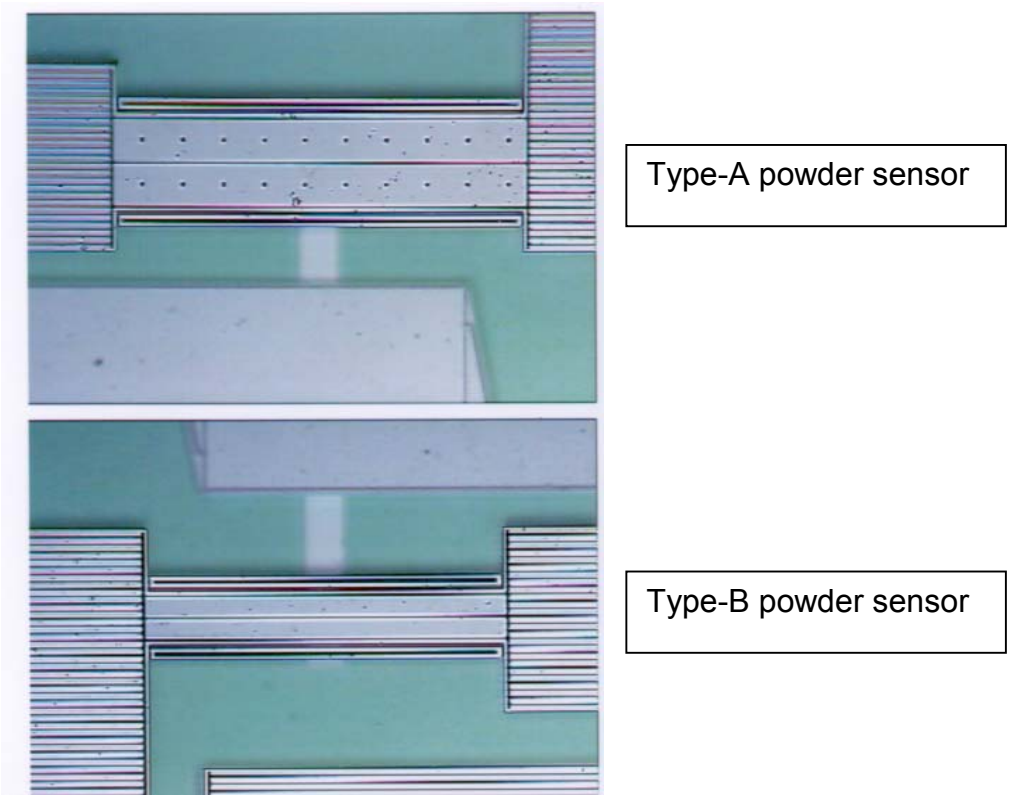

Figure 4- 10 Photographs of Type-A and Type-B powder sensors (same scale).

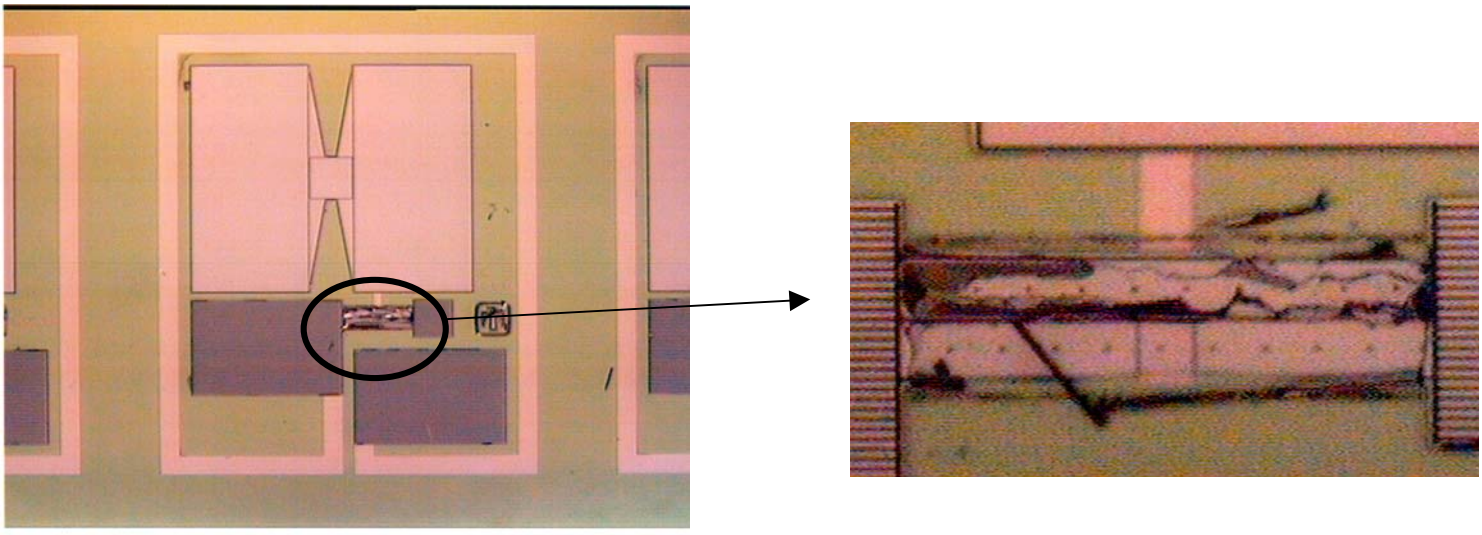

Figure 4- 11 Post-Pressing (5kpsi) photograph of smart SCB system with Type-A powder sensor. Note that damage is limited to powder sensor beam.

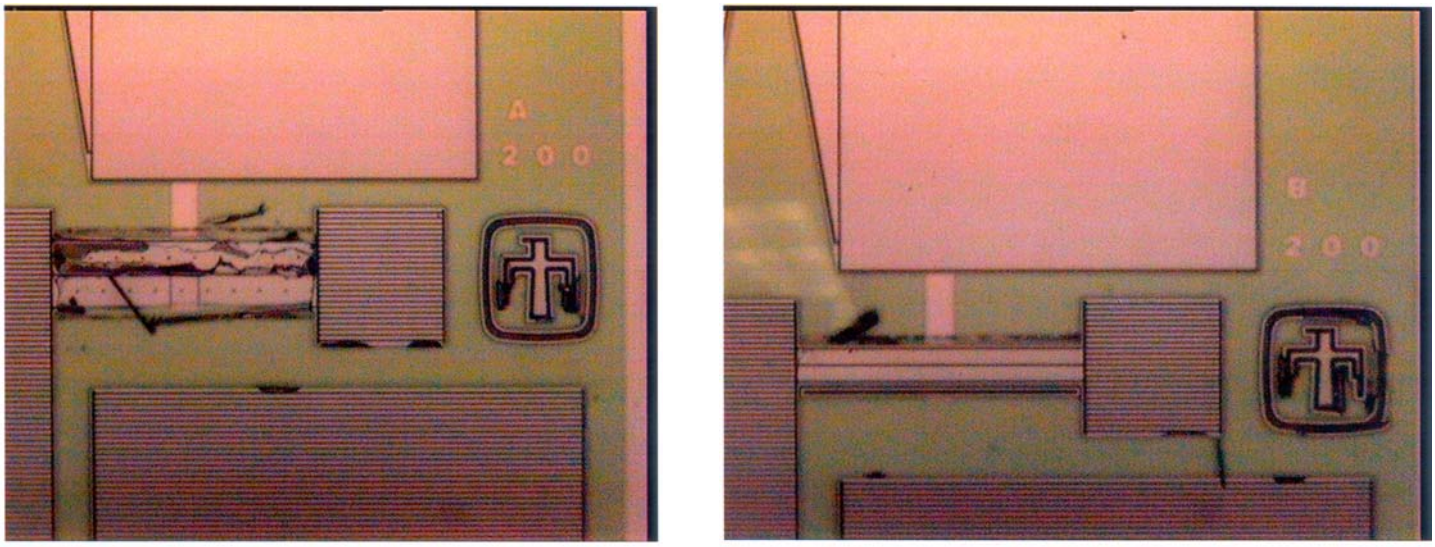

Figure 4- 12 Post-processing (10 kpsi) photographs of 200um-Type-A and 200um-Type-B powder sensors.

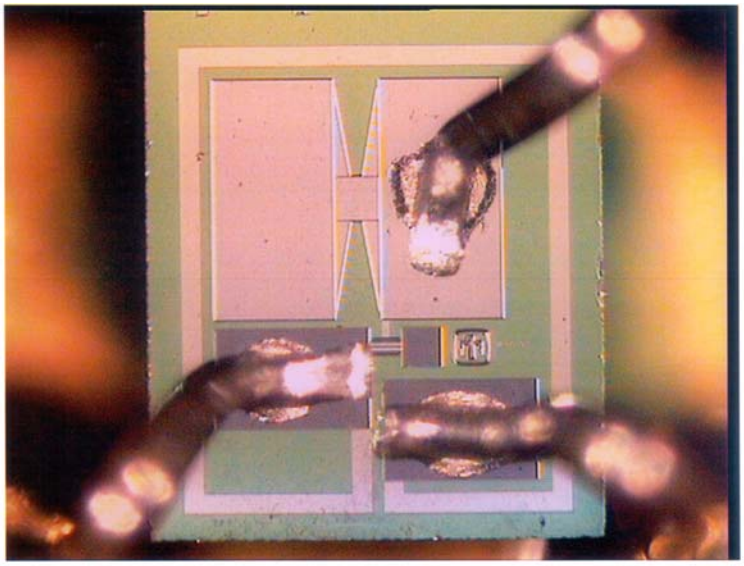

Figure 4- 13 – Single smart SCB die mounted and wire-bonded to header package.

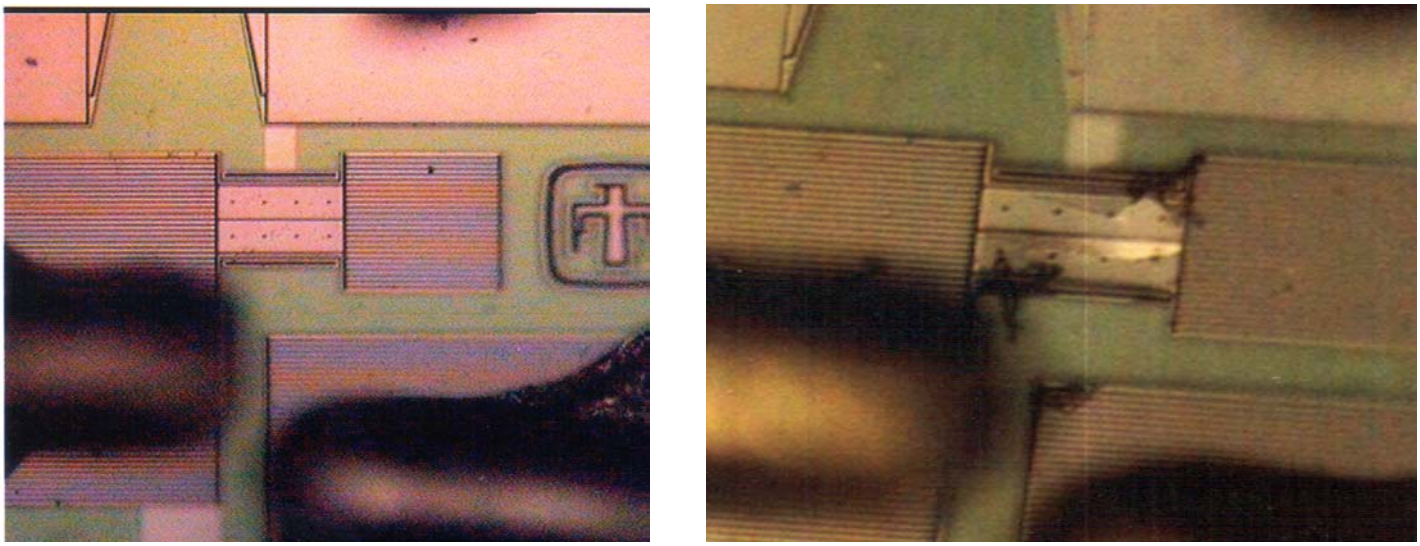

Figure 4- 14 Pre- and Post-pressing (8 kpsi) photographs of A75 powder sensor beam.

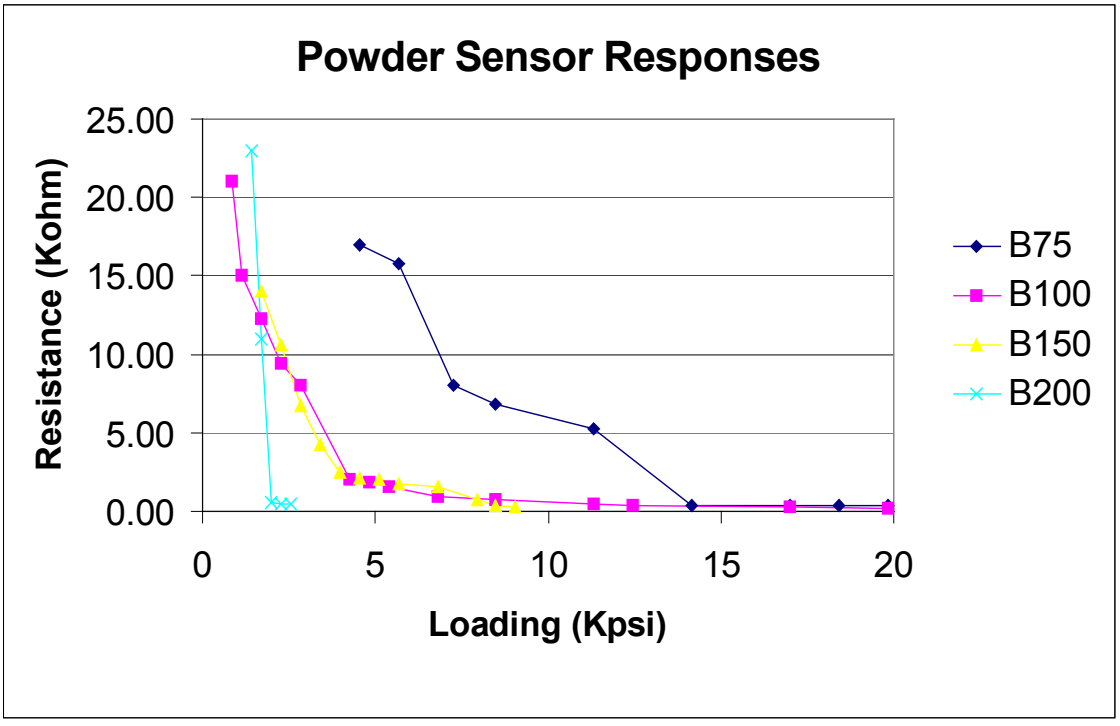

Figure 4- 15 – Powder sensor responses for various loading pressures.

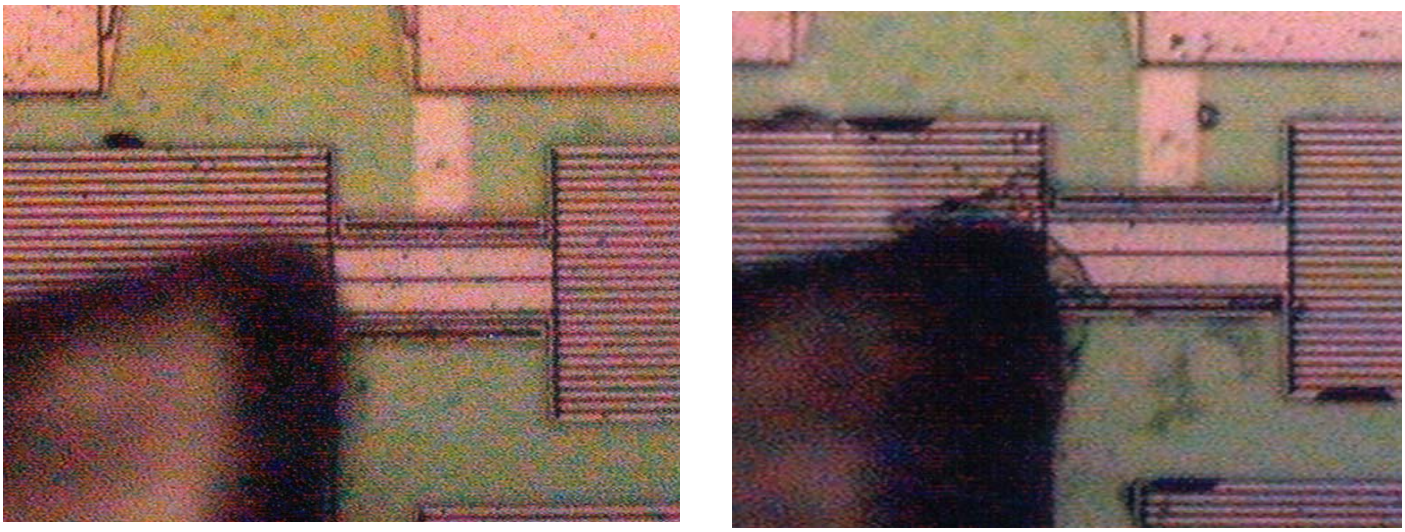

Figure 4- 16 Pre- and Post-pressing photographs of B75 powder sensor.

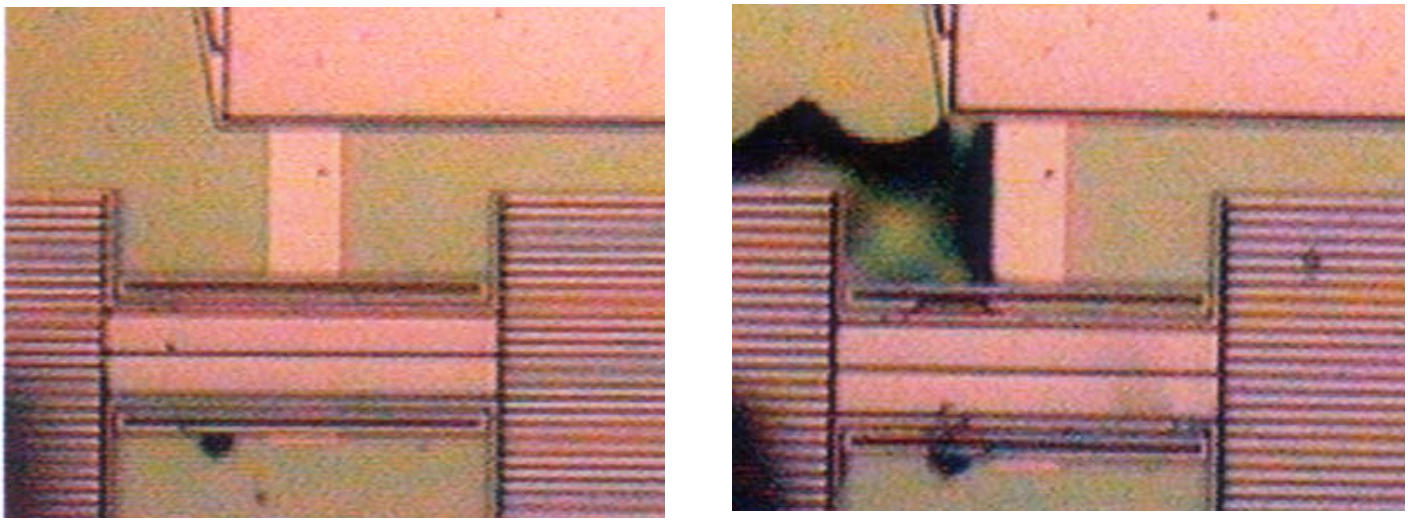

Figure 4- 17 Pre- and Post-pressing photographs of B100 powder sensor.

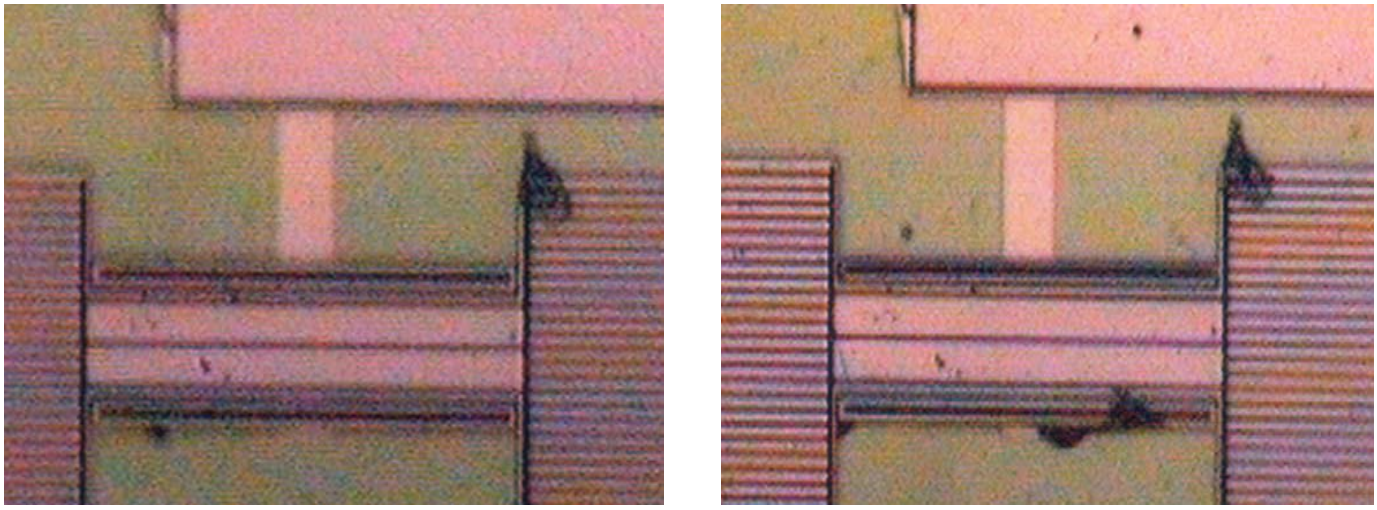

Figure 4- 18 Pre- and Post-pressing photographs of B150 powder sensor.

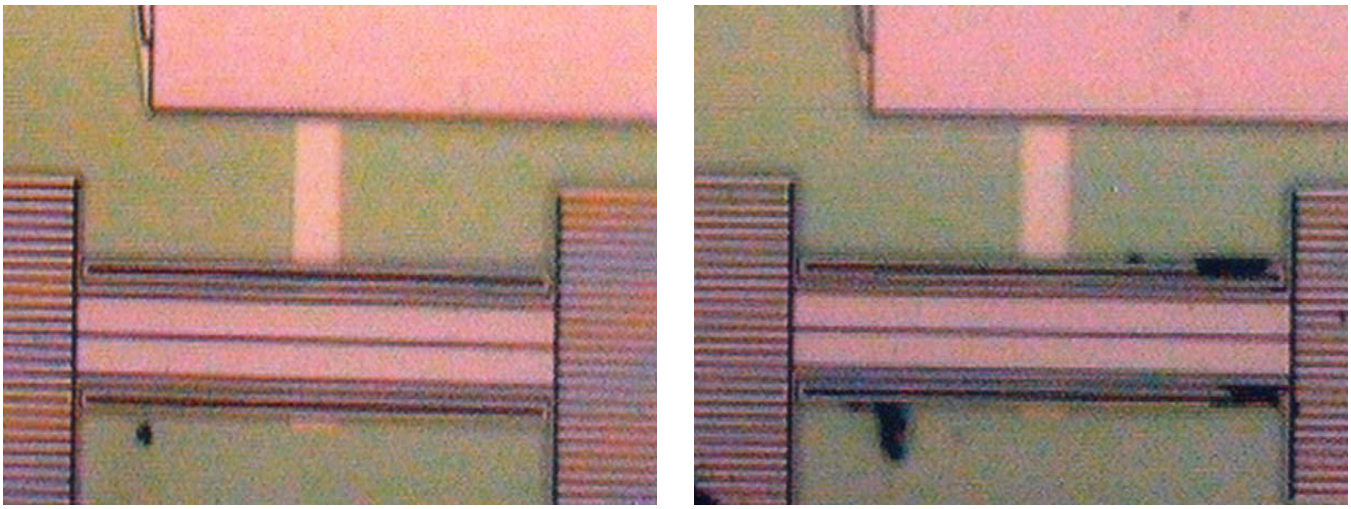

Figure 4- 19 Pre- and Post-pressing photographs of B200 powder sensor.

(THIS PAGE INTENTIONALLY LEFT BLANK)

DISTRIBUTION:

3 The Ensign-Bickford Company
Attn: Michael E. Alessio
660 Hopmeadow Street
P.O. Box 483
Simsbury, CT 06070-0483

3 SCB Technologies Inc.
Attn: Martin C. Foster
Bernardo Martinez-Tovar
1009 Bradbury Drive, S.E.
Albuquerque, NM 87106-4302

Analog Devices Inc.,
Attn: Daniel J. Savignon
7910 Triad Center Drive
Greensboro, NC 27409-9605

MS 0457 John H. Stichman, 2000
MS 0512 James K. Rice, 2500
MS 0513 Alton D. Romig Jr., 1000
MS 0521 Thomas J. Cutchen, 2501
5 MS 0614 Robert W. Bickes, Jr., 2523
MS 1071 David R. Myers, 1700
MS 1073 Wilson J. Barnard, 1736
MS 1084 Reid S. Bennett, 1748
MS 1452 Billy Marshall, 2552
MS 1453 Steven M. Harris, 2553
MS 1453 Gary W. Rivera, 2553
MS 1453 Gregory L. Scharrer, 2553
MS 1453 Stuart A. Smith, 2553
MS 1453 William W. Tarbell, 2553
MS 1454 Lloyd L. Bonzon, 2554
MS 1454 Mark C. Grubelich, 2554
MS 1454 Jill C. Miller, 2554
MS 1454 Anita M. Renlund, 2554
MS 1454 David E. Wackerbarth, 2554
MS 1380 Sheryl L. Martinez, 1323
MS 9018 Central Technical Files, 8945-1
2 MS 0899 Technical Library, 9616
1 MS 0612 Review and Approval Desk, 9612
For DOE/OSTI
MS-3180 CRADA Administrator, 1321